Journal of Archaeological Science 32 (2005) 1302–1327

Journal of Archaeological SCIENCE

http://www.elsevier.com/locate/jas

Geoarchaeology of Tyre's ancient northern harbour, Phoenicia

Nick Marriner [a,*], Christophe Morhange [a], Marcelle Boudagher-Fadel [b], Michel Bourcier [c], Pierre Carbonel [d]

[a] CEREGE, équipe de géomorphologie, Université de Provence, avenue R. Schuman, 13621 Aix-en-Provence, France
[b] Postgraduate Unit of Micropaleontology, Department of Geological Sciences, University College London, Gower St, London WC1E 6BT, UK
[c] COM, Station Marine d'Endoume, Université de la Méditerranée, 13006, Marseille, France
[d] CNRS, UMR 5805 EPOC, Université de Bordeaux I, Talence, France

Received 19 February 2004; received in revised form 21 March 2005

Abstract

Tyre's ancient northern harbour has been a source of scientific intrigue and debate for many centuries. Today an insignificant fishing harbour, looking north and sheltered from the dominant winds by a sandstone reef system, is all that remains of the famous Bronze Age, Phoenician, Hellenistic, Roman and Byzantine anchorage havens. In light of this many scholars have long questioned whether the modern port corresponds to its counterpart in antiquity. Here, we provide litho- and biostratigraphical evidence for an ancient harbour approximately twice as large as the present, comprising the modern day harbour and city centre. Four distinct sedimentary units have been identified, translating the different Holocene palaeoenvironments: (1) The Holocene transgressive contact is dated ca. 7800 BP, and lies at the base of a silty-clay lithodependant unit. Our proxies are consistent with a low energy, lagoonal type environment, protected by an extensive reef system. (2) Transition to a coarse sand fraction after ca. 5500 BP is concomitant with the accretion of a semi-protected pocket beach. This environment served as a proto-harbour during the Middle Bronze Age (MBA). (3) After the MBA, artificial harbour sedimentation is represented by a fine-grained silty-sand unit with stress on the natural biosystem. This unit attests to a closed, marine-lagoonal type environment, which existed until around 1500 BP. Dredging activity during the Roman and Byzantine periods explains the absence of 1st millennium BC strata. (4) The economic decline of the ancient city after the Byzantine period is marked by the opening of the basin to greater marine influence, with a progradation of the harbour coastline. Natural sediment infilling diminished the size of the harbour to its present dimensions, lost until now, beneath the Medieval and Modern centres.

Keywords: Ancient harbour; Geoarchaeology; Antiquity; Tyre; Lebanon; Eastern Mediterranean

1. Introduction

Located on the present day south Lebanese coastline, the ancient city of Tyre has been occupied by human societies since the Bronze Age [7,30]. Mother of Carthage and one of the greatest Phoenician city-states, Tyre's golden age spanned between the 9th to 6th centuries BC, during which period it enjoyed an extensive zone of influence incorporating large areas of the Mediterranean basin. Although Tyre lost its hegemony after 572/3 BC, when it fell under Persian influence [31], the city continued to prosper through the Hellenistic, Roman and Byzantine periods as attest the many impressive archaeological remains today visible in the city [15].

* Corresponding author.
E-mail addresses: nick.marriner@wanadoo.fr (N. Marriner), morhange@cerege.fr (C. Morhange), m.fadel@ucl.ac.uk (M. Boudagher-Fadel), bourcier@sme.com.univ-mrs.fr (M. Bourcier), carbonel@geocean.u-bordeaux.fr (P. Carbonel).

0305-4403/$ - see front matter © 2005 Elsevier Ltd. All rights reserved.
doi:10.1016/j.jas.2005.03.019

The search for Tyre's ancient northern and southern harbours has a long history of inquiry, beginning with early 17th to 19th century travellers and later pioneer archaeologists [23,47,58]. Whilst the position of the supposed southern harbour is an area of ongoing research and scientific debate [18], the modern day northern harbour, a sheltered bay looking north and protected from the dominant south-westerlies by a series of sandstone reefs, appears to correspond to its counterpart in antiquity. This has long posed problems to scholars, especially when one considers the small dimensions of the current day fishing harbour, a fact that seems largely disproportional with the former prominence of the 'Queen of the Seas' [8]. It is within this context that recent geoarchaeological study has centred (programs CEDRE F60/L58, UNESCO CPM 700.893.1 and AIST), seeking to reconstruct the palaeoenvironmental evolution of Tyre's northern harbour, in addition to its dimensions during antiquity [37]. The ability of multidisciplinary litho- and biostratigraphical techniques to resolve important archaeological and palaeogeographical questions has been demonstrated at numerous coastal sites including ancient Troy [33], Caesarea Maritima [56,57], Marseilles [40], Sidon [41] and Alexandria [26] to name but a few. In the absence of often expensive and technically difficult marine and terrestrial excavations, the geoarchaeological study of sedimentary harbour sequences is important for a number of reasons: (1) it enables the chronology of ancient harbours to be accurately established, notably with reference to their foundation; (2) it facilitates the spatial localisation of the basins and the reconstruction of their palaeogeographies; and (3) non-destructive geoscience techniques make it an innovative archaeological tool for the management and protection of very sensitive coastal sites.

2. Environmental context

Southern Lebanon's present geomorphological disposition has been fashioned by its position relative to the Arabian, Anatolian and African plates [12,17,60,64,70] (Fig. 1). A transform fault system between the Arabian and African plates has created extensive NNE/SSW strike-slip faulting. A second series of E-W cross-faults and folds, at the kilometre and 10 km scales, is attributed to collision between the Anatolian and African plates. The Tyrian peninsula occupies an uplifted NE/SW structural bloc, which is bound by the strike-slip displacements of the northern Arzai and the southern Zrariye fault systems [12]. During the Holocene, slip movement has led to a shallow downward displacement of the Tyre bloc relative to the two bounding structural blocs. This negative vertical displacement is corroborated by ancient urban quarters, quarries and a breakwater located along Tyre's southern coastal fringe, presently 2.5 m below mean sea level [18,42].

Pleistocene and Holocene coastal deposits characterise much of the Tyrian coastal plain. The original reef system upon which Tyre was founded, forms part of a series of Quaternary sandstone ridges, locally known as 'Ramleh', which run south to north along this sector of the continental shelf [6]. Ambiguity over Tyre's exact ancient physiography has resulted from numerous land reclamation projects undertaken since the Bronze Age. The defensive impregnability afforded by this 'island in the midst of the sea' (Ezek. 27:32) was eventually breached in 332 BC by the conquering armies of Alexander the Great. Alexander ordered the construction of a causeway, linking the island upon which the ancient city lay, to the continent. This feature significantly altered sediment deposition in the coastal zone between the island and mainland, and today the landscape is marked by a tombolo roughly 1500 m in length and 3000 m wide (on the continental side [Fig. 2]). Important sediment sources in the accretion of this tombolo have been the Litani river, which forms a delta just north of Tyre [1,2], with some questionable Nile clay inputs [44,67]. Recent research undertaken along the Israeli coast [63] and in the Saida area, southern Lebanon [59], has demonstrated the importance of sedimentary inputs from local fluvial systems.

Wave climatological data from the south-eastern Mediterranean coast show that only Tyre's north-eastern island corner is naturally protected from the dominant south-westerly swell and storm waves [13,14,27] (Fig. 2). This sector of the Mediterranean is characterised by extreme high energy sea-states with, for example, wave heights of more than 5 m being measured every ca. two years, and greater than 7 m every ca. 15 years [61].

3. Methodology

Our palaeoenvironmental reconstruction is based upon the litho- and biostratigraphical study of four core sequences deriving from the landward edge of the current northern harbour (Fig. 2, TI N 33° 16′ 412, E 35° 11′ 714; TII N 33° 16′ 389, E 35° 14′ 707; TV N 33° 16′ 391, E 35° 11′ 821; TIX N 33° 16′, 356, E 35° 11′, 818). Sediments were extracted using a 10 cm by 200 cm mechanised corer, with a protective metal sleeve mechanism lining the cored section. Preliminary core descriptions and log drawings were undertaken in the field, before analysis of the various lithoclastic and biological indicators under laboratory conditions. Cores were levelled by GPS and depths quoted on logs are relative to biological mean sea level, as represented by the upper limit of contemporary *Balanus* populations [34].

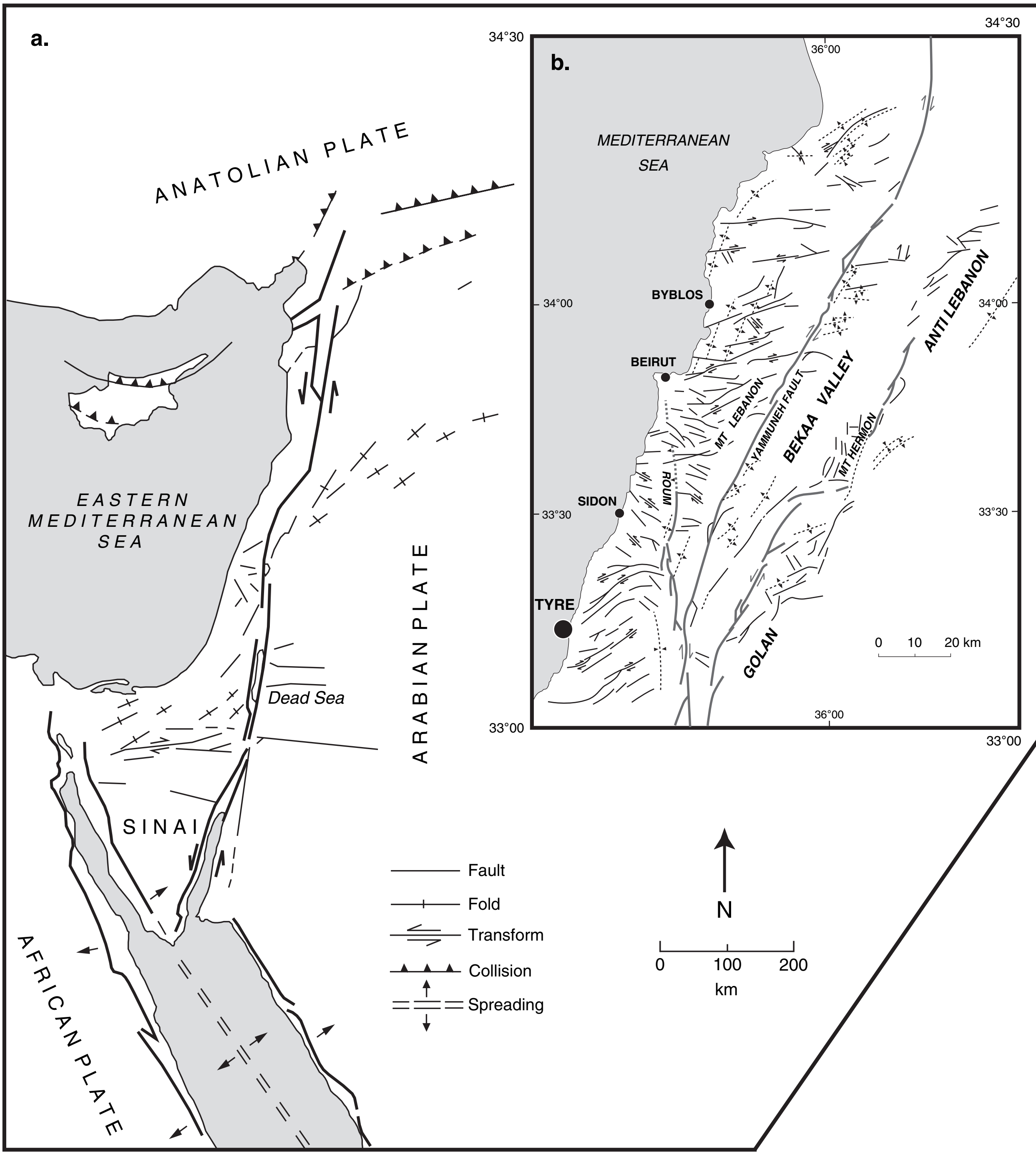

Fig. 1. (a) Plate tectonic setting of the Levant region (after Ron, 1987); (b) Lebanese fault system (after Dubertret, 1955).

The archives were stored in cold rooms prior to all laboratory analyses. Sediment samples were oven dried at 40 °C, the resultant dry aggregate being wet sieved to establish general texture. Two mesh sizes, 1.6 mm and 50 μm, were used to separate out the gravels and sand fractions. Macrofauna identification was undertaken upon the retained gravels fraction (> 1.6 mm) and assigned to assemblages according to the Péres and Picard [46], Barash and Danin [3], Poppe and Goto [49,50], Bellan-Santini et al. [5] and Bitar and Kouli-Bitar [9] classification systems. Microfauna (foraminifera [16] and ostracoda) were extracted from the sand fraction. The sand fraction also underwent mechanical sieving, sorted by 15 mesh sizes descending in size from 1.6 mm to 63 μm, and statistically analysed in concordance with various grain size parameters including histograms, fractiles and graphical indices [21].

The chronostratigraphy of the cores is constrained by a series of AMS radiocarbon determinations undertaken upon in situ marine macrofauna shells, charcoal

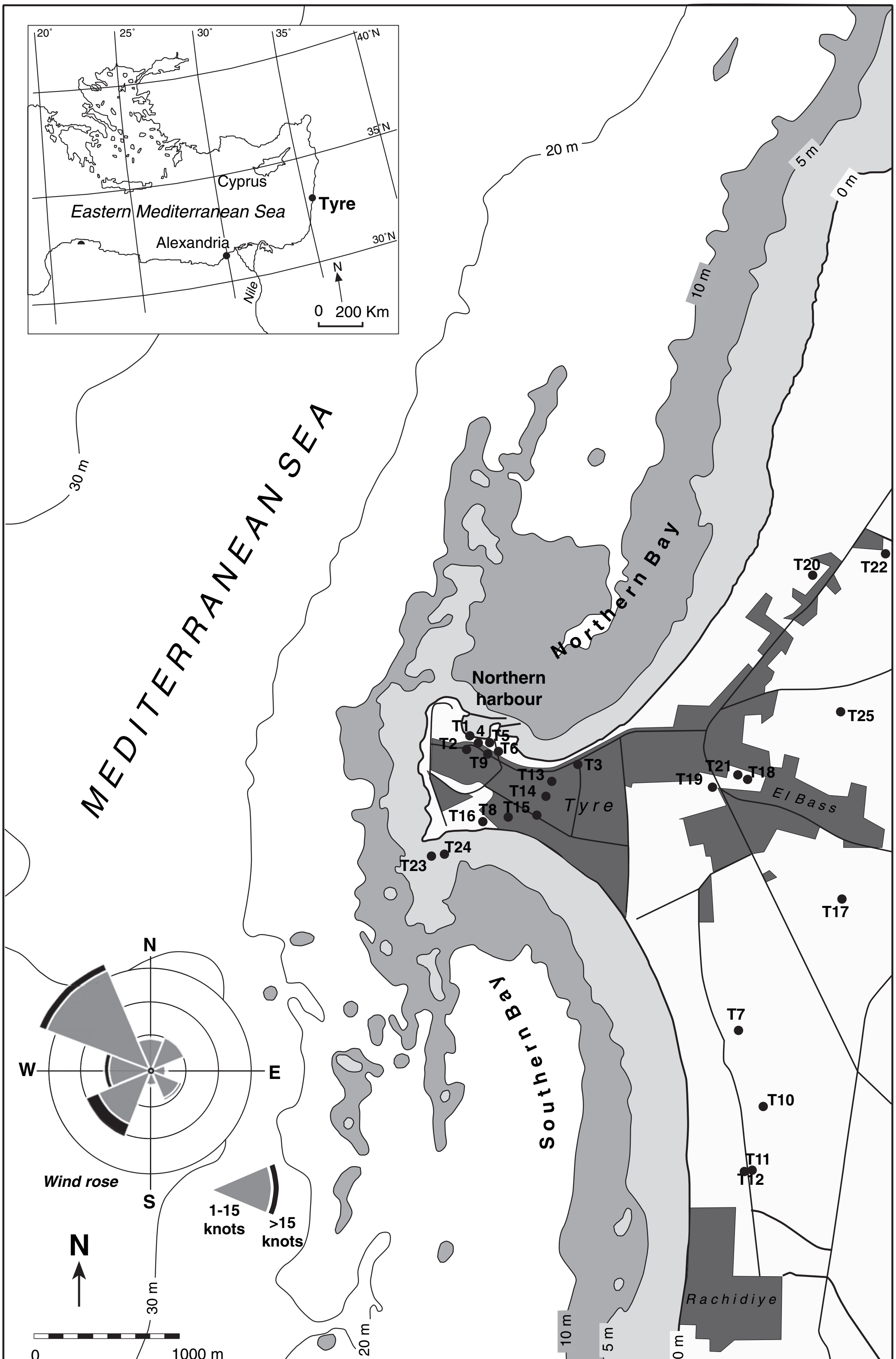

Fig. 2. Tyre, location of cores and coastal bathymetry. The strongest winds and swell derive from the south-west. Core sites are marked by a black dot.

fragments and seeds (Table 1). These were performed at the Centre de Datation pour le Radiocarbone at Université Lyon I, France and the Poznan Radiocarbon Laboratory, Poland. Determinations have been calibrated using Oxcal, and are quoted to two standard deviations. Material deriving from the marine domain has been corrected for reservoir effects of 400 years [55,66,68,69].

4. Results

Coastal stratigraphy and high-resolution laboratory analyses have enabled the ancient northern harbour of Tyre to be rediscovered. Here we report its palaeogeographical history since the flooding of the cove during the Holocene marine transgression.

4.1. Unit D – Marine transgressive unit ca. 8000 years BP

The Holocene depositional record begins with a shelly silt and clay transgressive contact dated 7800 ± 40 BP in core TV and 7840 ± 50 BP in core TIX (Figs. 3 and 4). Sediment texture indicates that unit D of TV and TIX is a lithodependent unit, in which marine litho- and bioclastic sedimentary inputs are incorporated into the reworked Ypresian clay substrate. The unit is dominated by upper muddy-sand (*Loripes lacteus*) and lagoonal macrofauna taxa (*Parvicardium exiguum*). High relative abundances of *Bittium reticulatum* are consistent with proximity to the reef system encircling the newly transgressed cove. This species prefers hard and sandy substrates, and its small size and cone-like morphology mean it is easily transported by marine currents.

Table 1
Radiocarbon determinations and calibration

Sample	Depth below MSL	Lab code	Material dated	$^{13}C/^{12}C$ (‰)	^{14}C BP	±	Cal. BP	Cal. BC/AD
TI 4	167.5	Lyon-1469 (GRA 17972)	*Cyclope neritea, Nassarius pygmæus, Ringicula auriculata*	1.14	1560	35	1210–1030	740 AD–920 AD
TI 12	207	Lyon-1470 (GRA 18730)	*Cyclope neritea, Haminea hydatis*	−0.31	1965	35	1600–1410	350 AD–540 AD
TI 30	307.5	Lyon-1472 (GRA 18732)	*Loripes lacteus, Tapes decussatus*	0.08	2255	35	1940–1770	10 AD–180 AD
TI 24	337.5	Lyon-1471 (GRA 19731)	*Cyclope neritea*	−1.4	2055	35	1700–1530	250 AD–420 AD
TI 31	342.5	Lyon-1602 (GRA 19345)	*Nassarius pygmæus*	0.89	2635	45	2430–2170	480 BC–220 BC
TI 36	367.5	Lyon-1603 (GRA 19346)	*Mitra cornicula*	0.94	5520	50	6000–5750	4050 BC–3800 BC
TI 39	382.5	Lyon-1473 (GRA 18733)	*Cyclope neritea*	−1.67	2375	35	2100–1910	150 BC–40 AD
TV 19	281.5	Poz-2500	Charcoal	−22.6	1485	30	1420–1300	530 AD–650 AD
TV 41	392.5	Poz-2502	Charcoal	−27.4	1910	30	1930–1770	20 AD–180 AD
TV 43	452.5	Poz-5768	Charcoal	−18.9	2265	30	2350–2150	400 BC–200 BC
TV 58	595	Poz-5752	*Nassarius mutabilis*	4.4	2360	30	2060–1890	110 AD–60 AD
TV 60	607.5	Poz-5769	Charcoal	−23.3	2245	35	2350–2150	400 BC–200 BC
TV 70	702.5	Poz-2445	*Cerithium vulgatum* juv.	2.8	5730	30	6240–6030	4290 BC–4080 BC
TV 76	737.5	Poz-2451	*Cerithium vulgatum* juv.	−1.2	6400	35	6970–6750	5020 BC–4800 BC
TV 77	740.5	Poz-2446	*Cerithium vulgatum* juv.	−1.5	7300	40	7840–7660	5890 BC–5710 BC
TV 81	752.5	Poz-2447	*Cerithium vulgatum* juv.	−4.1	7760	40	8330–8130	6380 BC–6180 BC
TV 82	755.5	Poz-2448	*Cerithium vulgatum* juv.	−2.4	7780	40	8340–8150	6390 BC–6200 BC
TV 106	827.5	Poz-2449	*Cerithium vulgatum* juv.	−5	7800	40	8350–8160	6400 BC–6210 BC
TIX 6	281	Poz-5770	Olive seed	−27.2	1615	30	1570–1410	380 AD–540 AD
TIX 20	387	Poz-5771	3 grape seeds	−26.9	1855	30	1870–1710	80 AD–240 AD
TIX 25	445	Poz-5773	2 *Nassarius mutabilis*	−0.8	2220	35	1900–1720	50 AD–230 AD
TIX 26	455	Poz-5774	Seed	−9.8	2385	30	2710–2340	760 BC–390 BC
TIX 35ch	545	Poz-5777	Charcoal	−21.3	2215	30	2330–2140	380 BC–190 BC
TIX 35co	545	Poz-5775	3 valves of *Loripes lacteus*	4.6	2505	30	2290–2080	340 BC–130 BC
TIX 43	630	Poz-5778	Seed	−24.8	2055	30	2120–1920	170 BC–30 AD
TIX 45	645	Poz-5779	Charcoal	−23.1	2320	35	2440–2150	490 BC–200 BC
TIX 49	679	Poz-5780	1 *Cyclope neritea*	3.5	2140	30	1810–1630	140 AD–320 AD
TIX 52	716	Poz-5781	3 valves of *Donax* sp.	2.9	2210	30	1880–1720	70 AD–230 AD
TIX 53	730	Poz-7184	2 valves of *Donax venustus*	−1.8	2300	30	1980–1830	30 BC–120 AD
TIX 62	829	Poz-5783	2 valves of *L. lacteus*	4.7	5850	40	6350–6170	4400 BC–4220 BC
TIX 63	838	Poz-5784	3 valves of *L. lacteus*	4.3	5830	40	6310–6160	4360 BC–4210 BC
TIX 76	963	Poz-5785	2 valves of *P. exiguum*	−1.6	7840	50	8390–8180	6440 BC–6230 BC

Examples of some of the molluscan species encountered are depicted in Figs. 5–7.

Unit D is dominated by the ostracod *Cyprideis torosa* which attains relative abundance figures of >80%. It indicates a sheltered, lagoonal type environment. Abrupt peaks of *Aurila woodwardii* and *Aurila convexa* are consistent with higher energy episodes, such as storms and high swell. Presence of the marine species *Loxoconcha* sp. indicates interaction with the open sea.

4.2. Unit C – Pocket beach unit (between ca. 5500 years and 2500 years BP)

Unit C of cores TI, TV and TIX is represented by a coarse sand facies (Figs. 3, 8 and 9). The onset of this unit is dated between 5520 ± 50 BP and 5850 ± 40 BP. The sand fraction predominates at between 40% to 90%, with sorting indices of 1.11 to 1.38, indicative of a mediocre sorted sediment. Skewness values between −0.03 and 0.53 are typical of a middle to low energy beach environment.

The macrofauna suites from all cores are consistent with a semi-sheltered environment, open to marine influence, in which both in situ taxa and imported individuals from other biocenoses are represented (Figs. 3, 10 and 11). The dominant taxa include reworked species from the hard substrate assemblage (*Cerithium rupestre*, *Fusinus pulchellus*, *Gibbula varia*), and in situ individuals from the upper-muddy sand in sheltered areas assemblage (*Nassarius corniculus*, *Cerastoderma glaucum*).

The semi-sheltered nature of the environment is corroborated by the microfossil biofacies (Figs. 4, 12 and 13). An increase in coastal species, notably *Aurila convexa*, is to the detriment of *Cyprideis torosa*. Presence of the marine-lagoonal taxa *Loxoconcha rhomboidea* and round *Xestoleberis* sp. do however indicate a relatively sheltered marine context. This unit corresponds to a semi-sheltered shoreface, consequence of the immersion of the Quaternary ridge at the end of the Holocene marine transgression. Numerous marine taxa including *Semicytherura* sp., *Bairdia* sp., *Cistacythereis* sp., *Jugosocythereis* sp., *Loculicytheretta* sp., and *Callistocythere* spp. are drifted in and corroborate communication with the open sea. The foraminifera indicate a sandy marine depositional context. *Patellina corrugata*, *Cibicides* spp., *Gyroidinoides* spp., and *Nonion* spp. are concurrent with a shallow environment, less than 10 m in depth [43].

4.3. Unit B – Ancient harbour

Unit B comprises two fine muddy-sand facies, B1 and B2, clearly differentiated by the litho- and biostratigraphical signatures.

4.4. Unit B2 – Artificial Roman harbour

In unit B2, silts and clays comprise 2% to 22% of the total dry sediment weight, sands constituting 59% to 92% and the gravels 2% to 30%. Unimodal histograms well developed in the finer end of the scale, and skewness values of −0.16 to −0.52, indicate a relatively low energy depositional environment. The unit is characterised by a series of radiocarbon dates which cluster between ca. 2000 BP and 2400 BP, with a number of age-depth inversions. We interpret this as evidence of harbour dredging during the Roman period (see Section 5).

The molluscan faunas continue to be characterised by taxa from diverse biocenoses. Despite the increasingly sheltered nature of the environment, marine currents persist in importing extra situ species. Those taxa deemed in situ are dominated by species from the upper clean-sand assemblage (*Cyclope neritea*, *Smaragdia viridis*, *Nassarius pygmaeus*, *Nassarius mutabilis*) and the upper muddy-sand assemblage (*Macoma cumana*, *Haminea hydatis*, *Loripes lacteus*).

Three taxa dominate the ostracod fauna in TI: *Loxoconcha* sp., round *Xestoleberis* sp. and *Aurila convexa*. *Loxoconcha* sp. and round *Xestoleberis* sp. both prefer muddy to sandy substrates, and have oligo-mesohaline salinity ranges [38]. They indicate a marine-lagoonal environment. Continued exposure to outer marine dynamics is manifested by low percentages of marine species such as *Cushmanidea* sp. and *Aurila woodwardii*. In TV, presence of the brackish-lagoonal species *Loxoconcha elliptica* is consistent with a sheltered harbour in connection with the open sea (Fig. 4). Coastal taxa such as *Urocythereis oblonga* and *Aurila convexa* are also present in significant numbers.

The foraminifera are dominated by shallow water species such as *Amphistegina* spp. *Peneroplis planatus* is common in the unit and translates a sheltered marine environment with low levels of water action.

4.5. Unit B1 – Artificial Byzantine harbour

Unit B1 is dated between ca. 1500 BP to 2200 BP, a chronology corresponding to the Byzantine period. The unit is characterised by a low energy, fine muddy-sand facies. The sedimentological indicators are all consistent with an exceptionally sheltered harbour environment existing up until the 6th to 10th centuries AD.

Increased confinement relative to B2 is indicated by a fall in macrofauna and microfauna species diversity. In core TI, sharp rise in *Cerithium vulgatum* (up to 70% of the unit's macrofauna content), which prefers hard substrates in areas of silt and clay accumulation, appears concomitant with stone-based harbourworks such as moles and quays. Other in situ taxa include individuals from the upper clean-sand assemblage

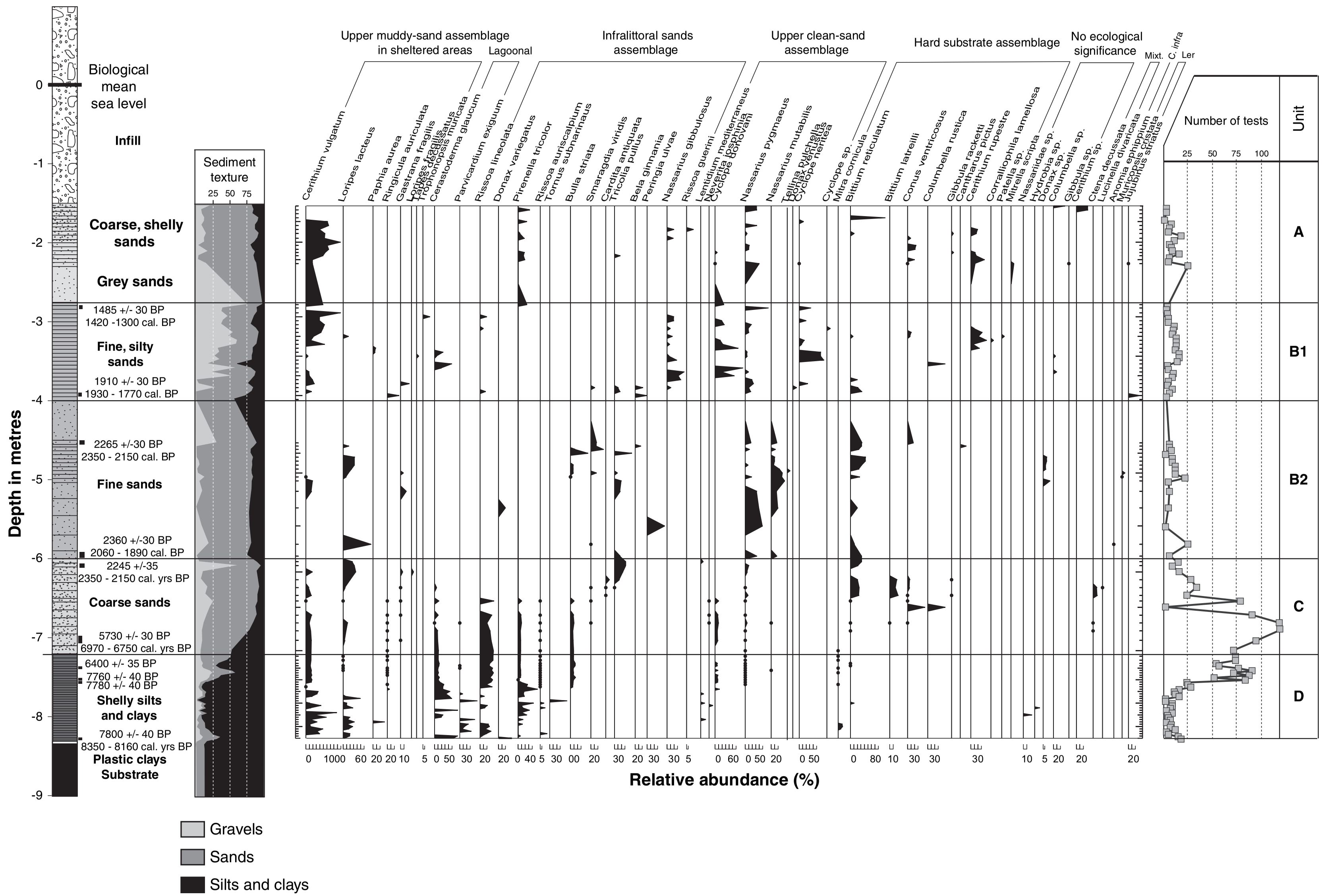

Fig. 3. Macrofauna core TV.

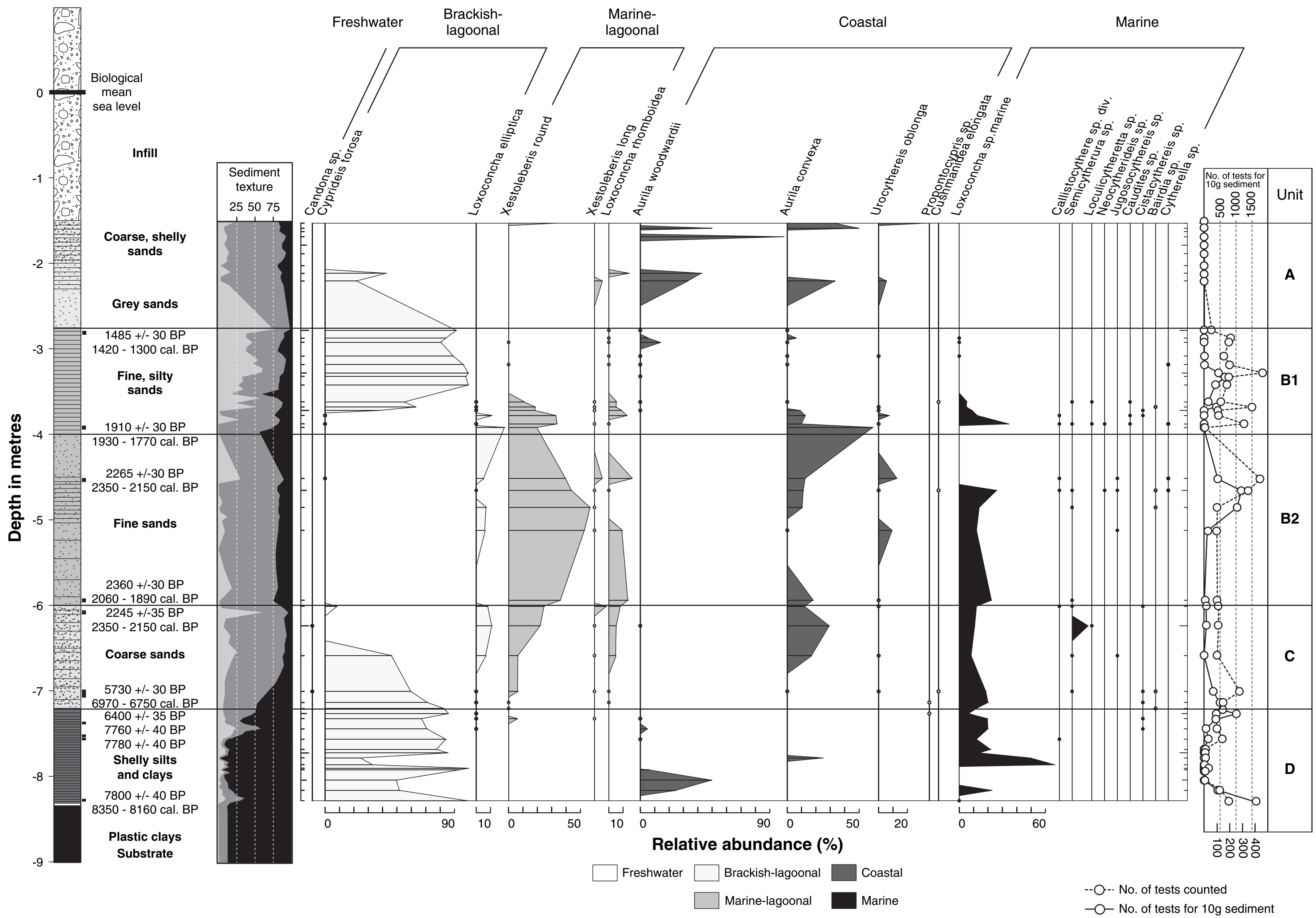

Fig. 4. Ostracoda core TV.

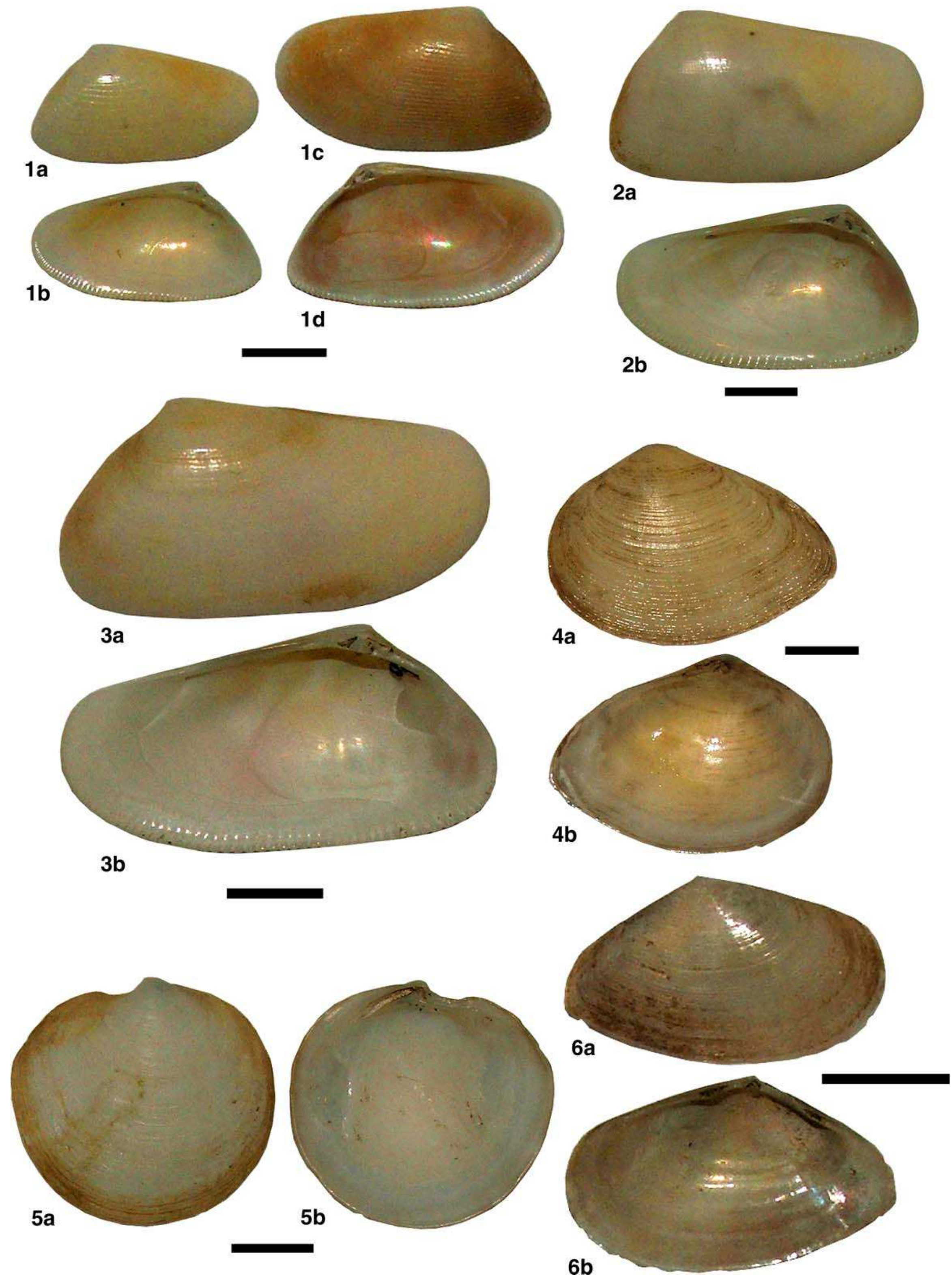

Fig. 5. Scale bar: 5 mm. 1a–d: *Donax semistriatus*; 2a–b: *Donax trunculus*; 3a–b: *Donax venustus*; 4a–b: *Gastrana fragilis*; 5a–b: *Loripes lacteus*; 6a–b: *Tellina donacina*. Photos by N. Marriner.

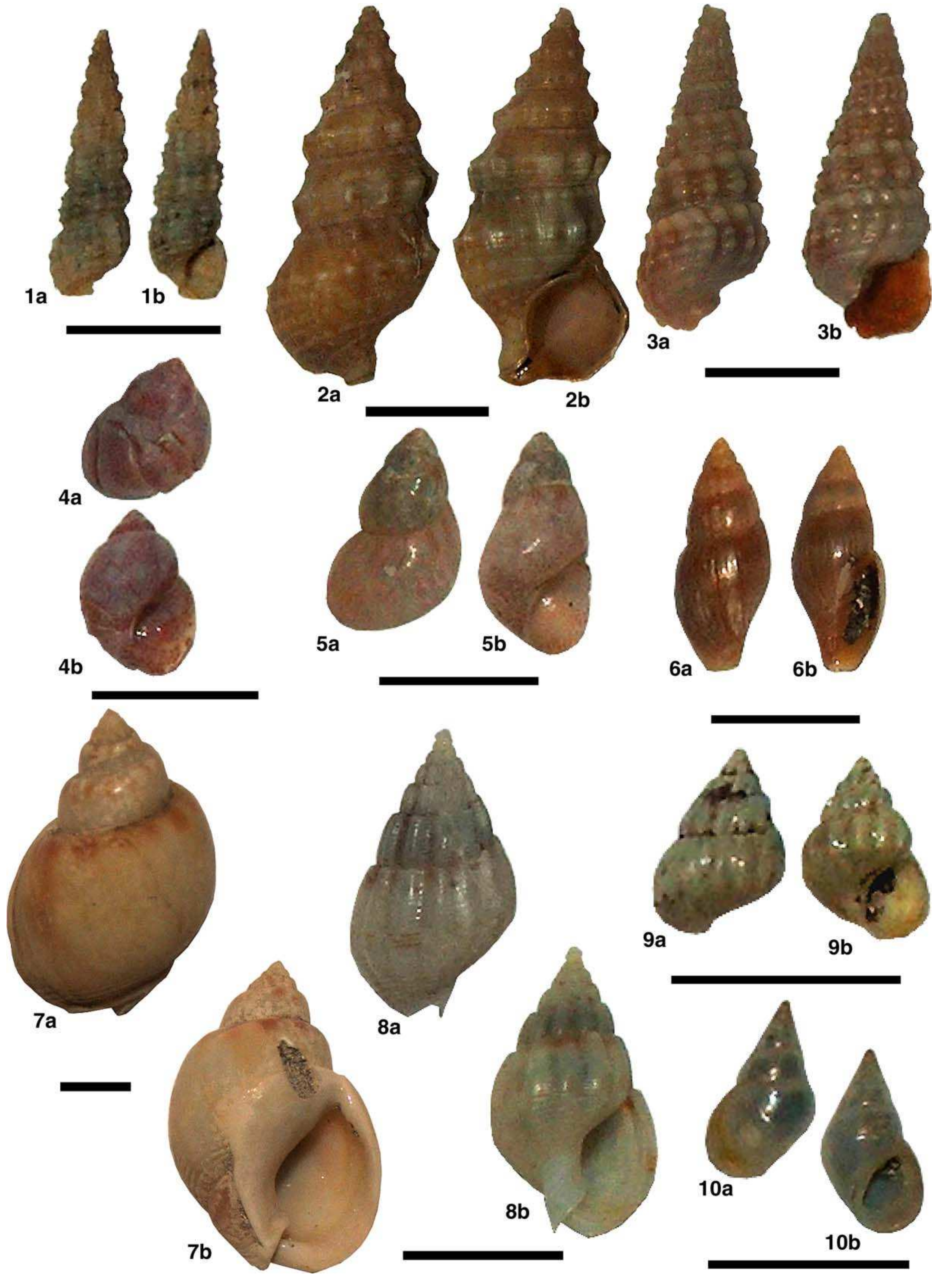

Fig. 6. Scale bar: 5 mm. 1a–b: *Bittium reticulatum*; 2a–b: *Cerithium vulgatum*; 3a–b: *Pirenella conica*; 4a–b: *Tricolia pullus*; 5a–b: *Tricolia tenuis*; 6a–b: *Mitra ebenus*; 7a–b: *Nassarius mutabilis*; 8a–b: *Nassarius pygmaeus*; 9a–b: *Rissoa lineolata*; 10a–b: *Rissoa monodonta*. Photos by N. Marriner.

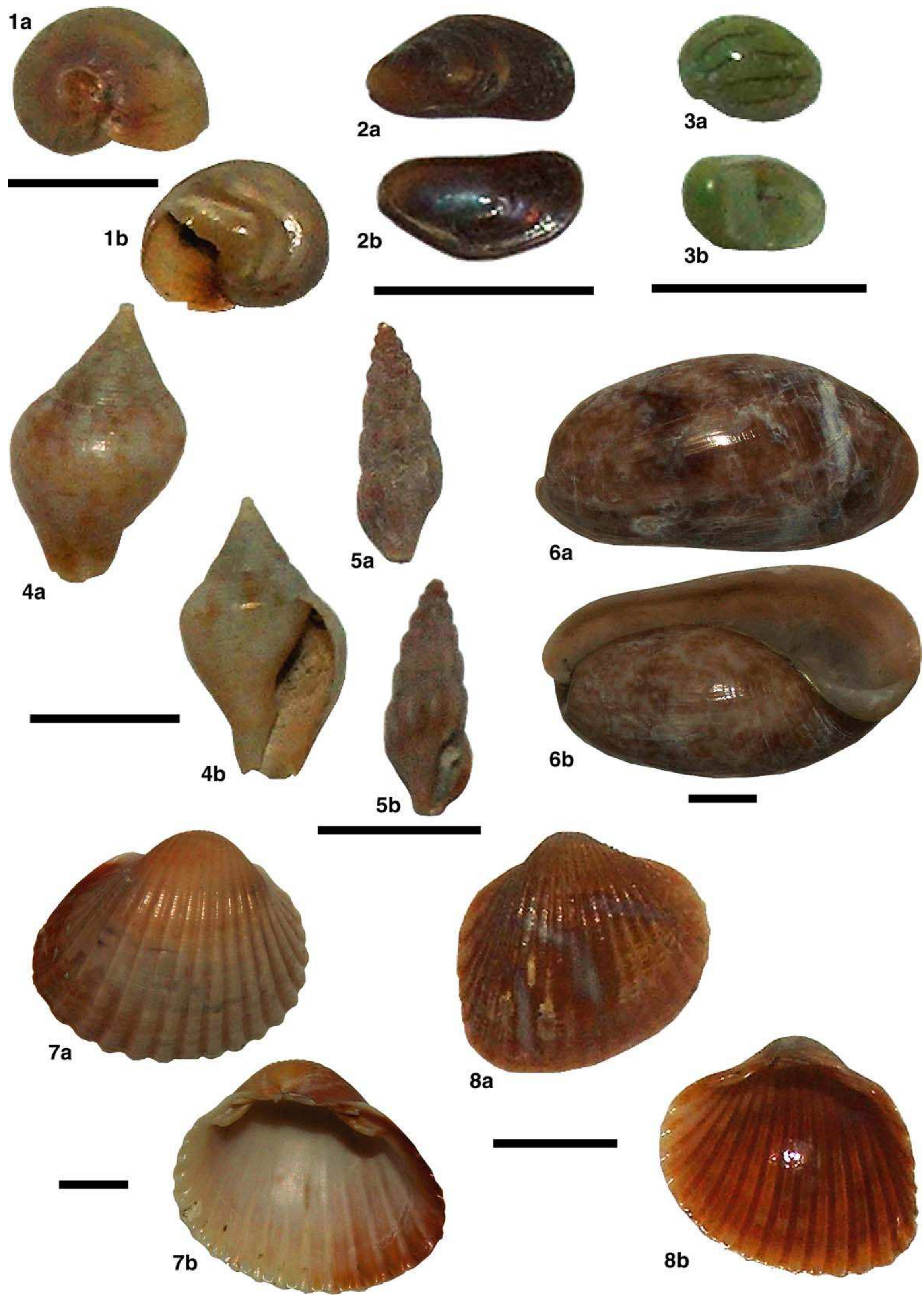

Fig. 7. Scale bar: 5 mm. 1a–b: *Cyclope neritea*; 2a–b: *Mytilaster minimus*; 3a–b: *Smaragdia viridis*; 4a–b: *Columbella rustica*; 5a–b: *Bela ginnania*; 6a–b: *Bulla striata*; 7a–b: *Cerastoderma glaucum*; 8a–b: *Parvicardium exiguum*. Photos by N. Marriner.

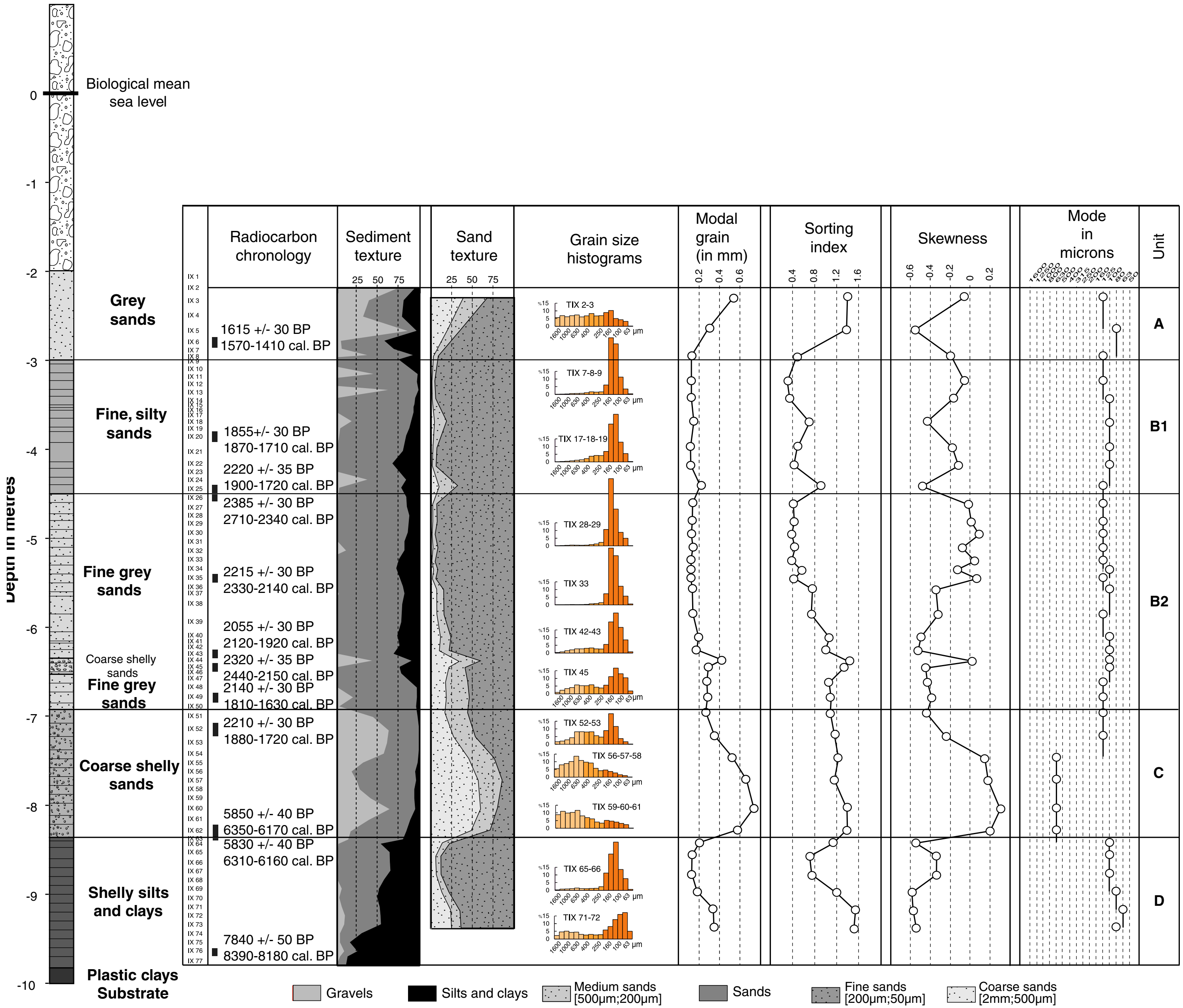

Fig. 8. Grain size analyses core TIX.

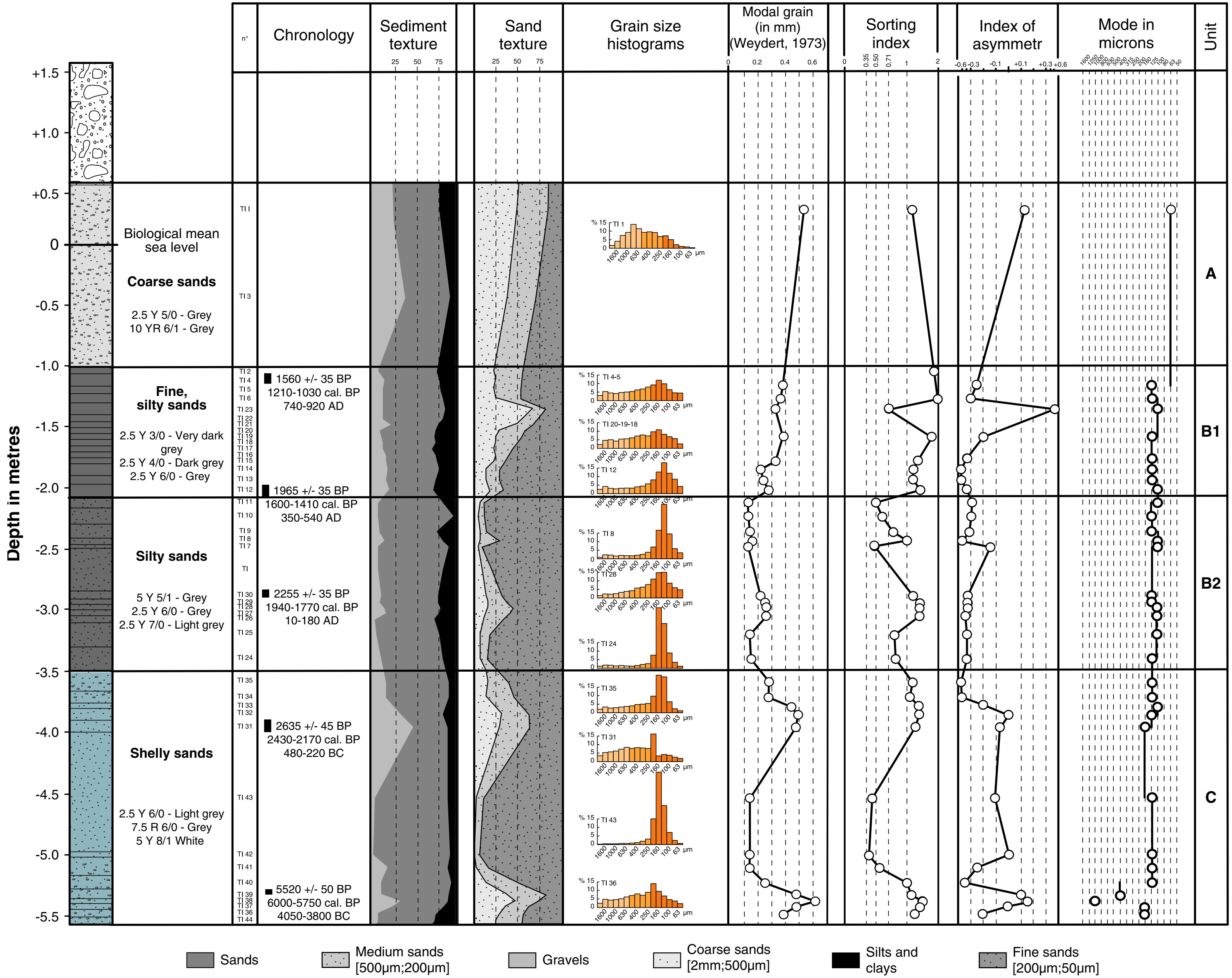

Fig. 9. Grain size analyses core TI.

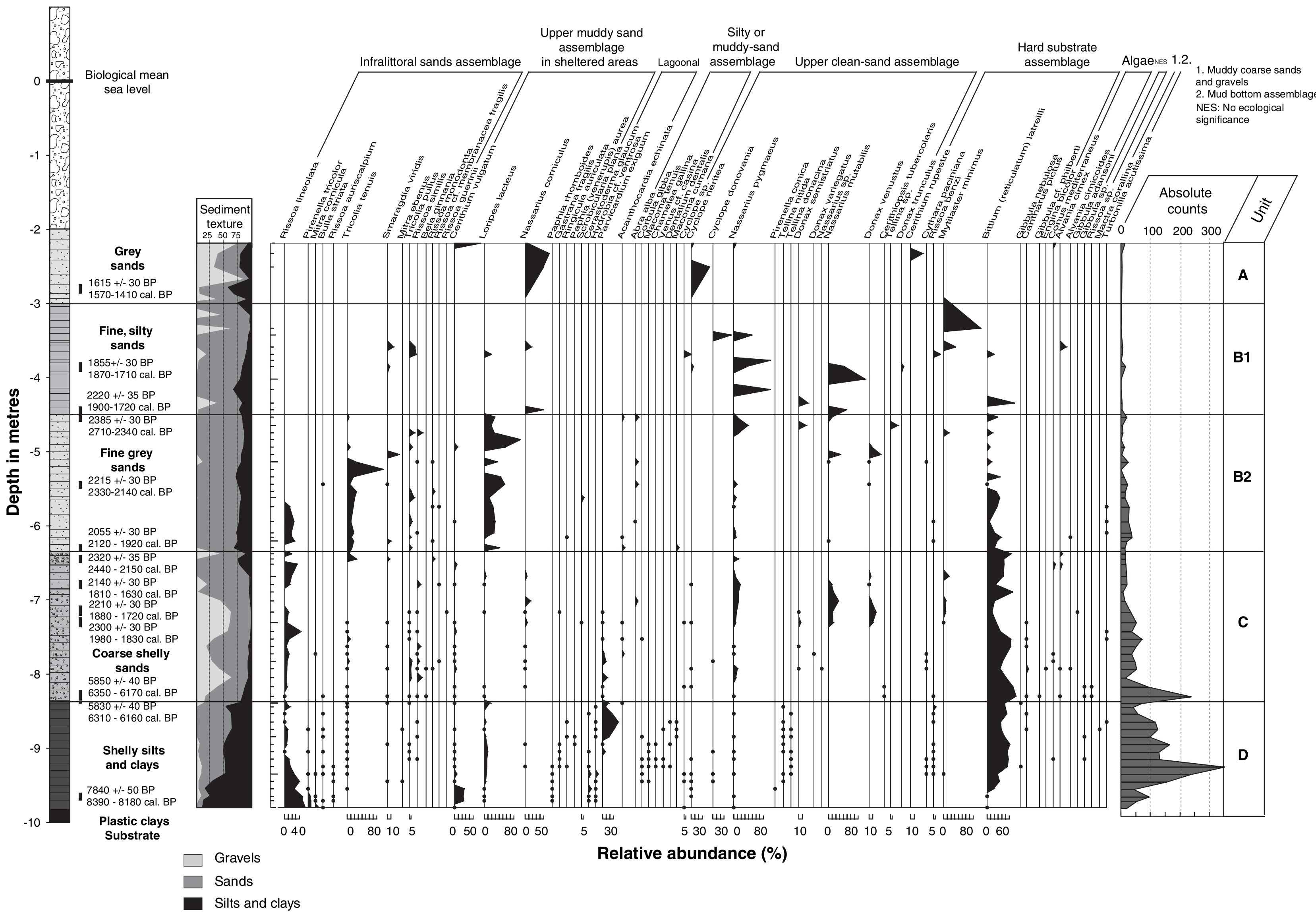

Fig. 10. Macrofauna core TIX.

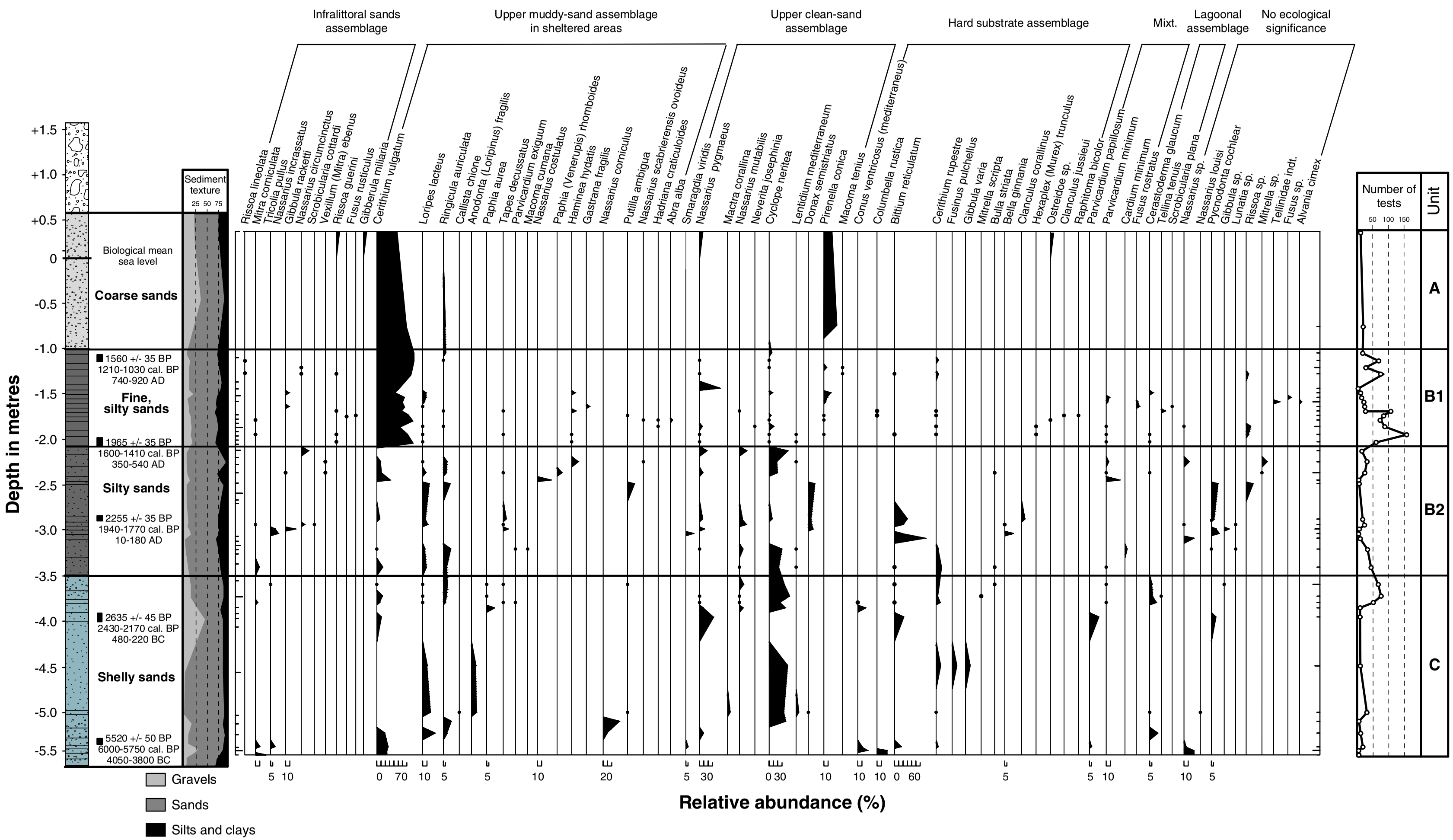

Fig. 11. Macrofauna core TI.

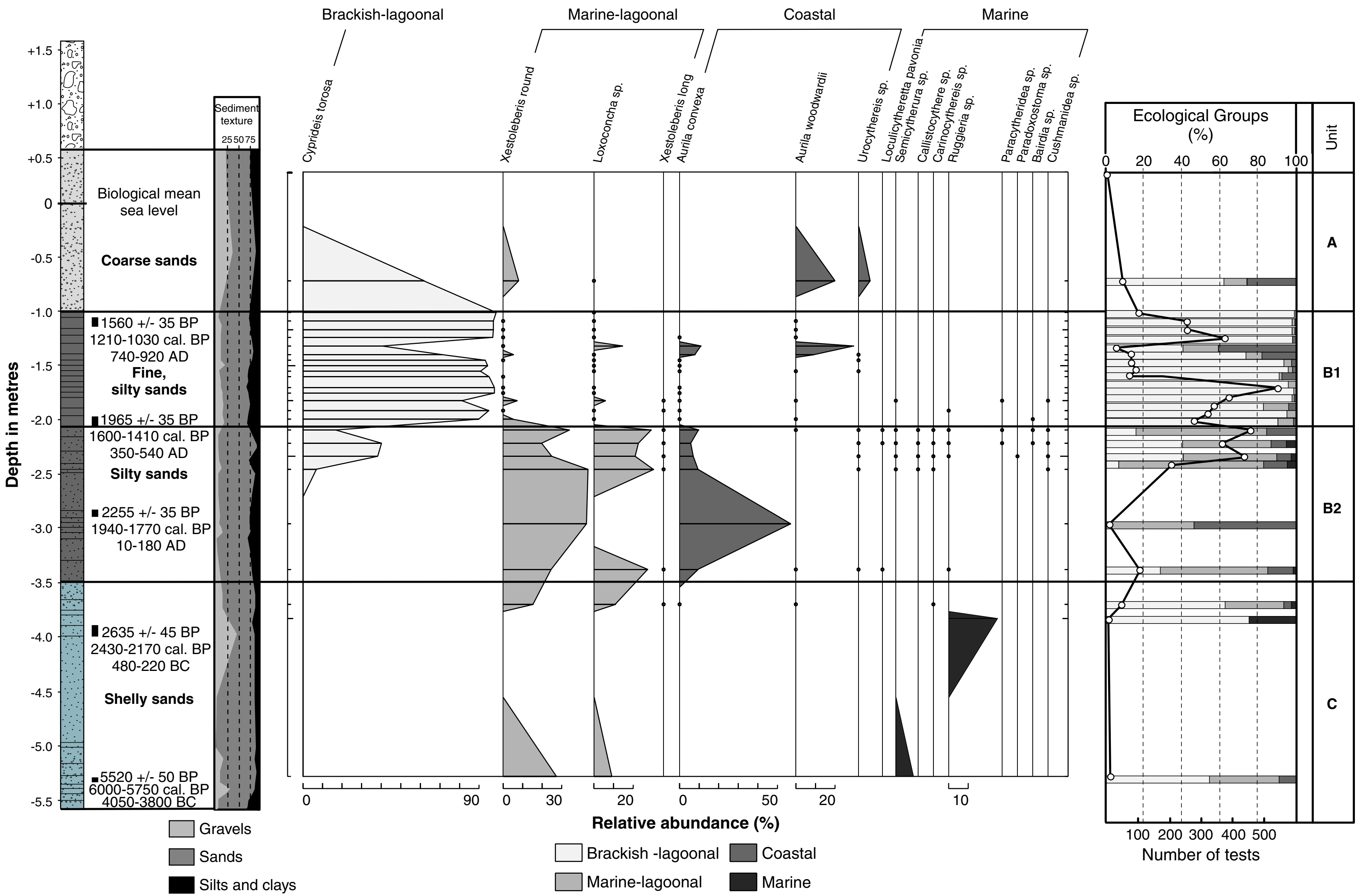

Fig. 12. Ostracoda core TI.

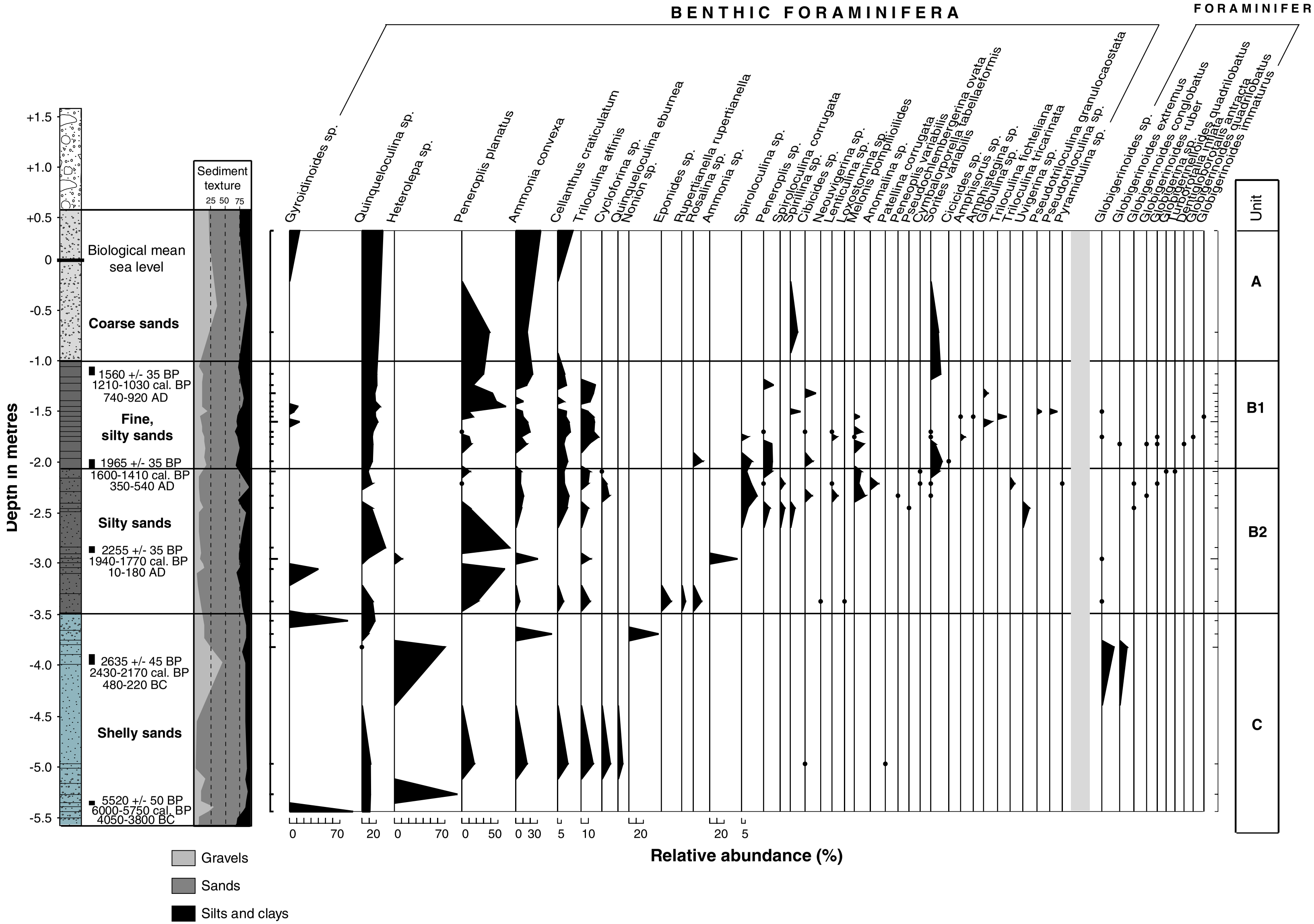

Fig. 13. Foraminifera core TI.

(e.g. *Pirenella conica*, *Cyclope neritea*), the lagoonal assemblage, and the upper muddy-sand assemblage in sheltered areas.

For the ostracoda, *Cyprideis torosa* attains relative abundance figures in excess of 90% and is associated with a sheltered restricted to leaky lagoon (i.e. a very well-protected harbour [32]). Absence of outer marine species is a result of confinement from the open sea. The porcelaneous foraminifera species, *Peneroplis planatus,* and *Ammonia convexa* dominate this unit. Presence of these forms, together with *Sorites variabilis* and *Cellanthus craticulatum* corroborate a sheltered, shallow hyposaline environment [29,28,62].

4.6. Unit A – Exposed beach environment (post-Byzantine)

The transition to unit A is dated to between the 6th to 10th centuries AD. The unit comprises a grey, shelly sand unit with textures of between: 3% to 31% for the gravels, 58% to 83% for the sands and 9% to 18% for the silts and clays.

Cerithium vulgatum and *Pirenella conica* dominate the macrofauna suite, with numerous secondary species from diverse biocenoses (*Ringicula auriculata*, *Nassarius pygmaeus*, *Gibberula miliaria*), consequence of an environmental opening. The increase in coastal ostracod taxa such as *Urocythereis* sp. and *Aurila woodwardii*, is to the detriment of the formerly abundant lagoonal taxa of unit B. This translates a re-exposure of the environment to the influence of the marine swell and currents. For the foraminifera, the dominant taxa are *Ammonia convexa*, *Peneroplis planatus* and *Cellanthus craticulatum*. The tests of many of these individuals have been broken by wave action, confirming a rise in energy dynamics, due to the collapse of harbour maintenance. This is linked to the demise of Tyre as a Mediterranean commercial centre.

5. Discussion

Between ca. 8000 BP and 6000 BP, our litho- and biostratigraphical indicators attest to a relatively shallow, low energy marine environment, newly transgressed by the post-glacial sea-level rise. These data are consistent with published 'eustatic' sea-level curves [4,19]. The lithology is marked by a high proportion of fine sands and silts, concomitant with reworking of the underlying clay substratum. Bio-sedimentological data indicate a protected environment, shelter afforded by the proximal aeolianite ridges, yet to be completely submerged by the transgressing waterbody. With contemporary sea level approximately 8–12 m below present [20], the bathymetry indicates that the sub-aerial extension of the sandstone ridges forming Tyre island had a greater northerly and southerly extension. Such a physiography sheltered the cove from dominant onshore south-westerly winds and swell. Small peaks of extra situ ostracod taxa, from the coastal and marine domains, were imported during periods of heightened swell.

After the onset of relative sea-level stability around 6000 BP, the northern coast of Tyre remained naturally semi-protected by the small aeolianite ridges and offshore reef system (Fig. 14). Until the first millennium BC, the bio-sedimentological proxies of the Tyrian Bronze Age basin were typical of a semi-open marine cove. The linear, shelter-less Levantine coast yielded few such geomorphological contexts, and our data suggest that this natural pocket beach served as a proto-harbour to early mariners and settlers on the island. Shallow draught boats would have been hauled onto the beach-face, with more sizeable merchant vessels being anchored in the bay [35]. In the northern harbour of Sidon, a similar sandy proto-harbour phase is dated to the Middle Bronze Age (MBA), ca. 3600 BP (1700–1450 cal. BC [41]). Questions concerning the existence of artificial harbourworks during the MBA are an area of ongoing debate. Along the northern Levantine coastline, Frost [22] attributed the early harbour infrastructure of Arrados (Arwad, Syria) to the Bronze Age. A harbour quay in Dor, Israel, has been constrained to the 14th–13th BC [53,54]. The MBA site of Yavne-Yam, Israel, also shows the presence of boulder piles on a submerged ridge, used to improve the quality of the ancient anchorage [36]. In Tyre, only archaeological excavations would permit unequivocal corroboration of our geoarchaeological data.

We interpret the absence of 1st millennium BC strata (Phoenician to Hellenistic periods), as evidence of dredging during the Roman and Byzantine periods. The semi-protected Phoenician harbour would have been characterised by accelerated accretion rates and silt enrichment. Linear regression, performed on the radiocarbon dataset for dates spanning the Hellenistic to Byzantine periods, indicate average accretion rates of ca. 10 mm/yr, compared to 0.5 to 1 mm during the proto-historic period. Persistent age-depth anomalies within the fine-grained harbour facies are consistent with repeated dredging activity through the Roman and Byzantine periods (Fig. 15). Stratigraphic evidence for dredging practices is known from the ancient harbours of Marseilles and Naples. In Marseilles, two Roman dredging boats, dating from the 2nd and 3rd centuries AD, were excavated by Pomey [48]. In Naples' ancient harbour, extensive dredging activity is recorded from the 4th century BC.

The litho- and biostratigraphical facies of the cores indicate two continuous phases of confinement. The first phase corresponds to the Roman period and the second to the Byzantine epoch. The fine-grained sedimentation

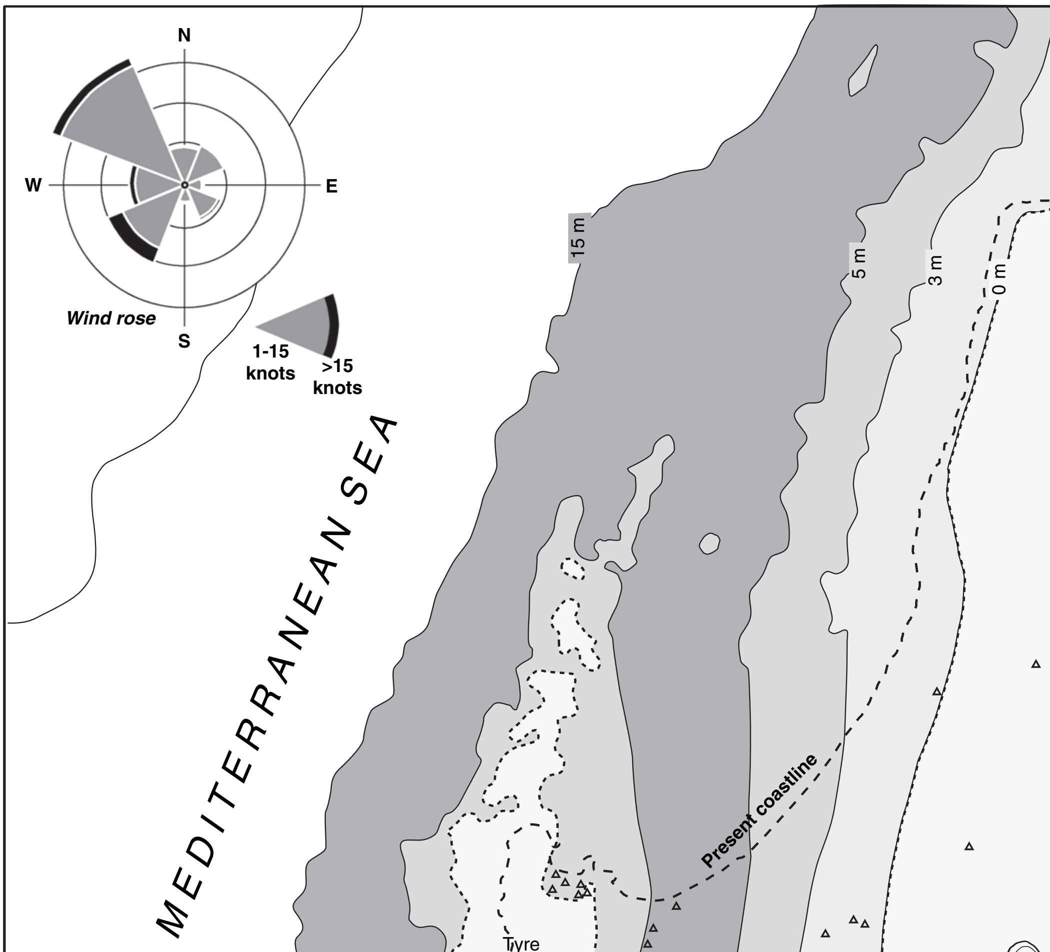

Fig. 14. Reconstructed palaeobathymetry of Tyre around 6000 years BP. Coastline reconstructed using stratigraphy, present bathymetry and geochronology.

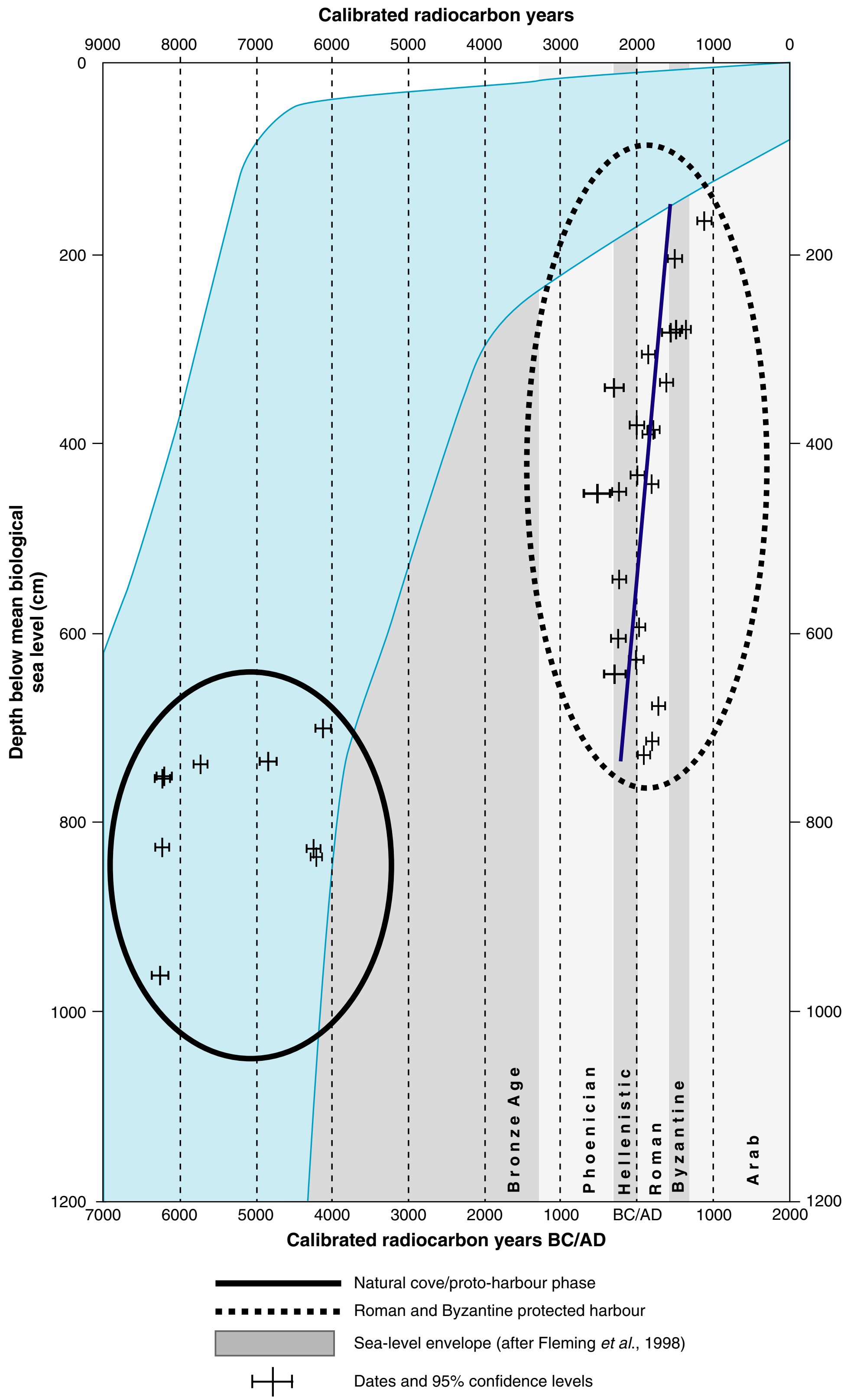

Fig. 15. Age-depth plot of radiocarbon dates from Tyre's ancient northern harbour. All depths are given relative to present biological mean sea level.

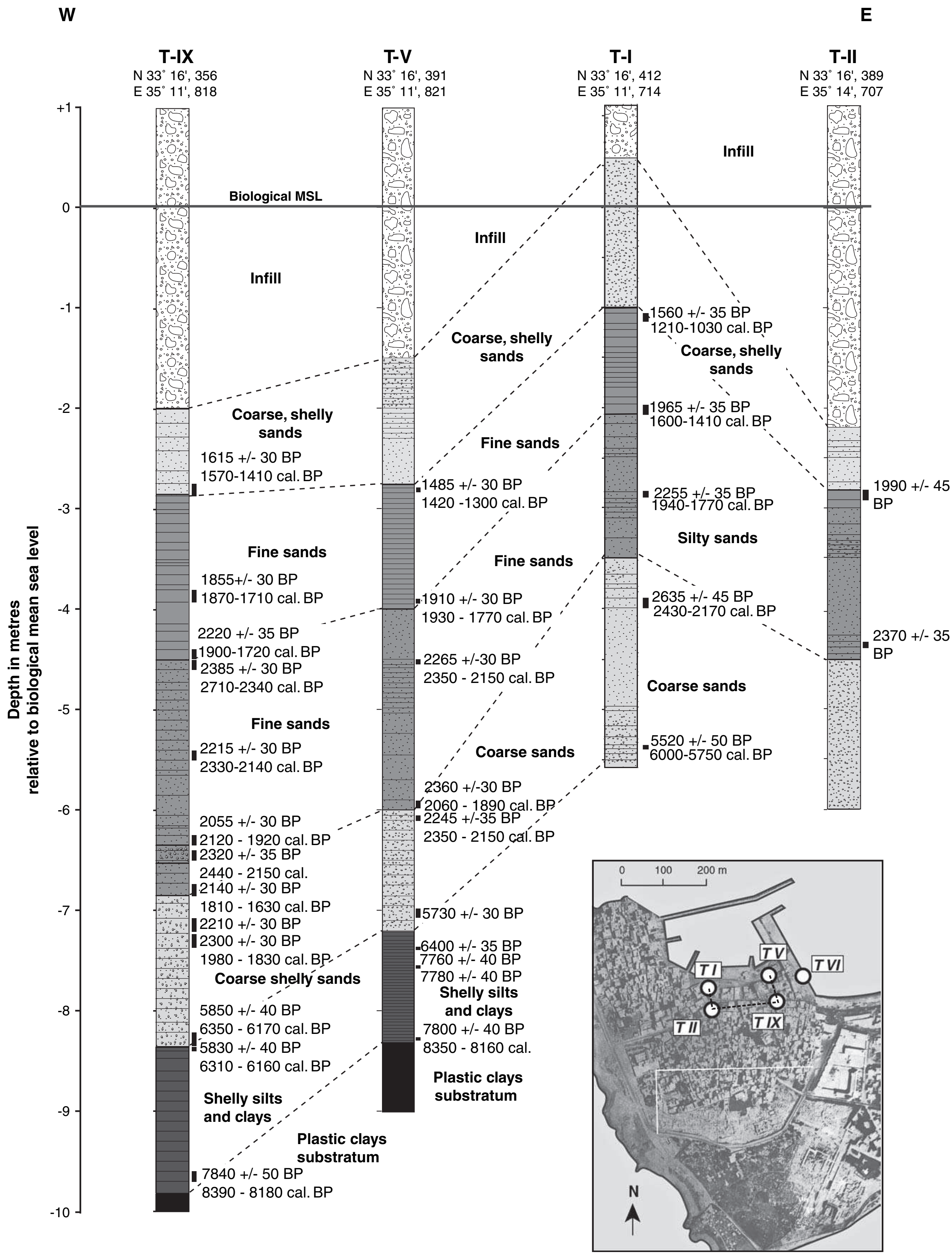

Fig. 16. Cross-correlation of stratigraphic units from cores in the northern harbour.

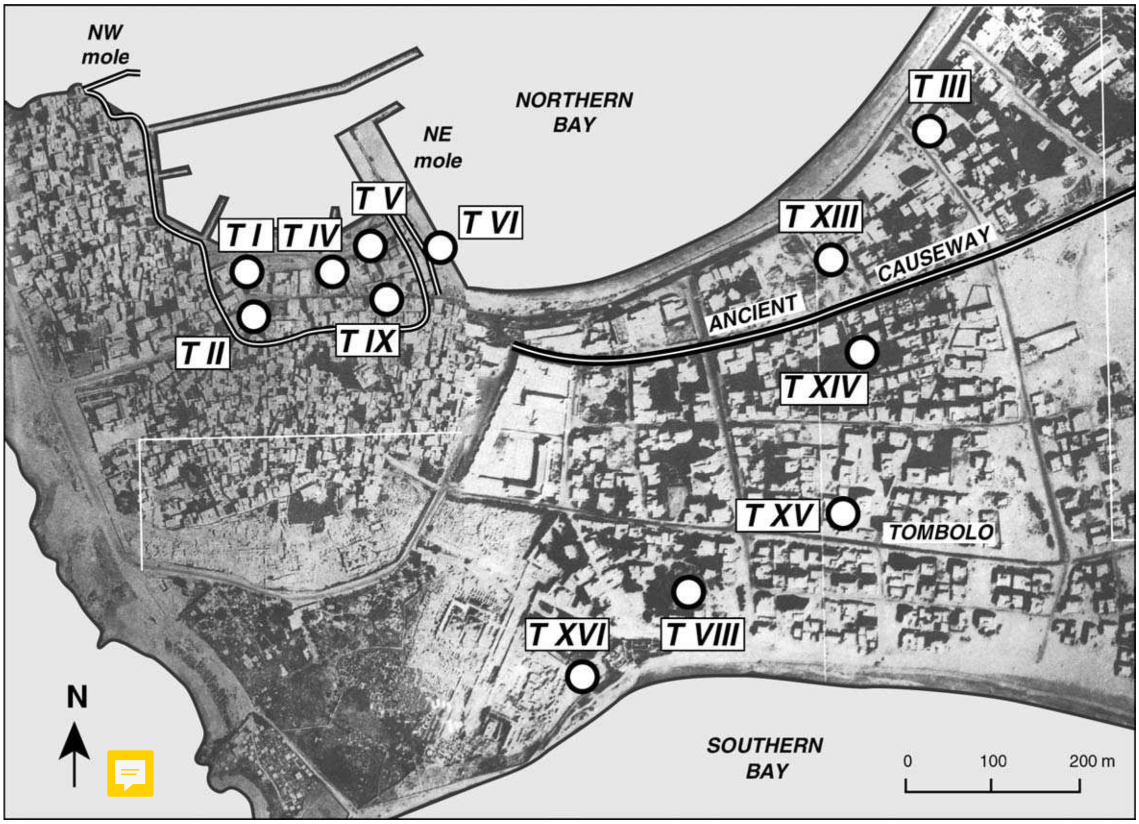

Fig. 17. Maximum extension of Tyre's MBA northern harbour (1950s aerial photograph). Our work reveals the ancient harbour was ca. 40% larger than present, the extra surface area lying beneath the Medieval and Modern city centres.

Fig. 18. Tyre's northern harbour in 1799 (by J.F. Cassat, mission de Bonaparte en Egypte et en Orient).

and environmental stress observed are typical of ancient harbour depositional contexts with a properly controlled entrance from the open sea [25,39]. The ancient harbour acted as a sediment sink accumulating a long sequence of fine-grained silts, clays and organic matter. Sediment provenances include wadi and river inputs from the north, notably the Litani, and south of Tyre [59]. The importance of Nile sediments in this sector of the Levant is an area of scientific contention, with some researchers arguing for a dominant Nile provenance [44] whilst others believe local sediment sources have played a more important role during the Holocene [63,67]. Pending mineralogical analyses of the harbour sediments and modern day sediment analogues from the Tyre sector, will shed greater light on this question.

Although artificial harbourworks created the low-energy conditions conducive to fine-grained sedimentation, it is also important to underline three critical changes since the Bronze Age, which all contributed to a rise in sediment yields. (1) The use of mud-bricks in ancient construction yielded clay particles through runoff along streets converging on Tyre's northern harbour [11]. (2) The beginnings of land clearance and agriculture in the Levant are dated ca. 4500–3500 BP [10,71], creating upstream soil erosion crises and accelerated sediment accumulation in low energy base-level environments. (3) Finally, ancient harbours were used as huge waste dumps. For example, the coarse harbour sediment fractions consist of numerous species of wood, leather, ceramics and reworked macrofauna.

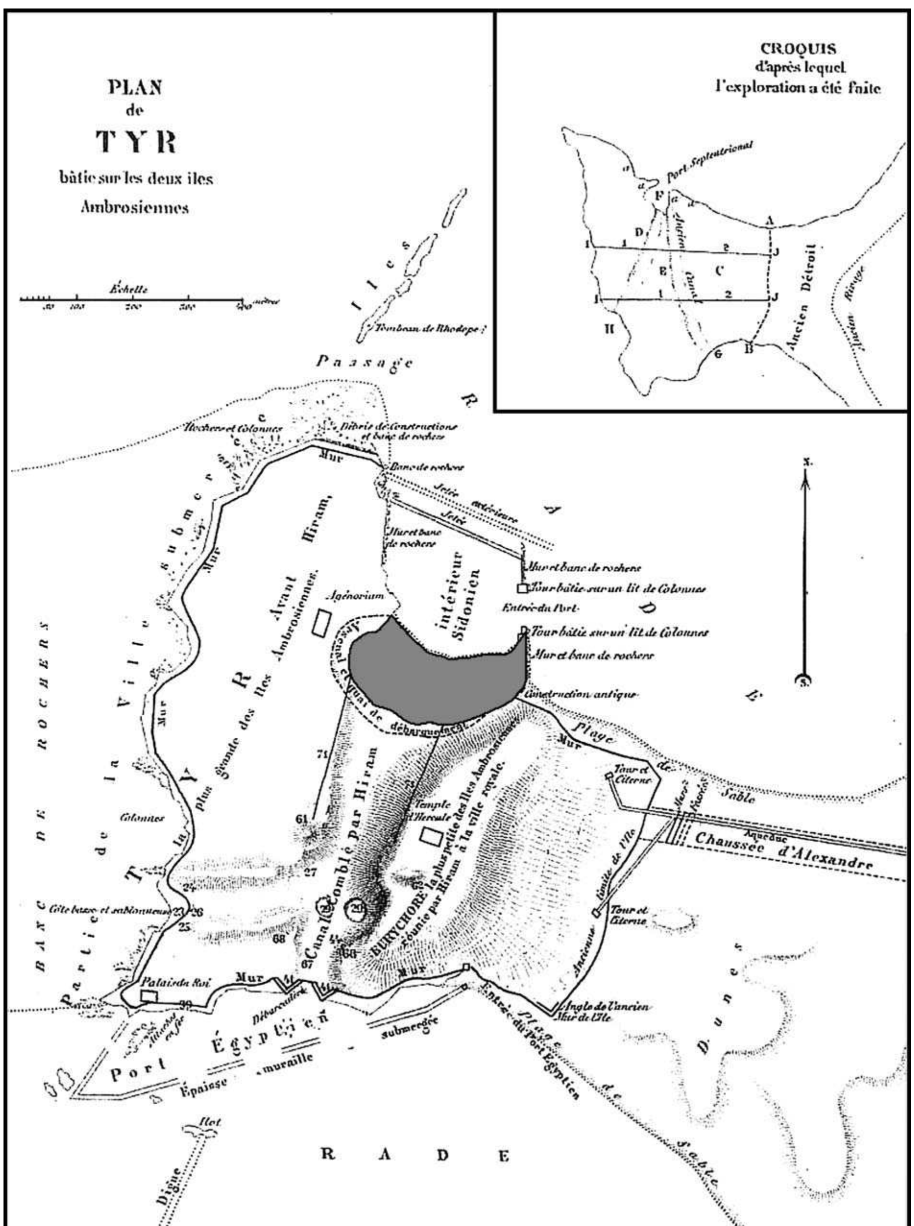

Fig. 19. Map of ancient Tyre as proposed by Poulain de Bossay (1863).

A later phase of increased harbour confinement is recorded during the Byzantine period, and is consistently observed throughout the harbour stratigraphy (Fig. 16). The exact reason for this period of accentuated confinement is most probably the result of a change in harbour management techniques during the Byzantine period. It appears to correspond to the harbour apogee, as in other ancient Levantine ports [57,65].

The economic decline of Tyre is clearly translated in the northern harbour stratigraphy by an exposed beach unit, a classic feature of all abandoned ancient harbours [25]. Deteriorating infrastructure no longer shelter the ancient harbour confines, and we observe a progradation of the coastline after the 6th to 10th centuries AD.

High-resolution topographical surveying, urban morphology, coastal stratigraphy, old photographs, gravures and archaeological diving allow us to precisely determine the maximum extension of the northern harbour, corresponding to the MBA. It was twice as large relative to present, with a large portion of the former basin lying beneath the modern market (Fig. 17). On the seaward side, the western sandstone ridge has spatially constrained the harbour in this direction. An important portion of the former basin is today located between the present-day breakwater and its ancient submerged counterpart [24,45]. This long-term progradation tendency explains the comparatively diminished size of the modern day fishing harbour relative to antiquity. To the east, core TVI, deriving from just beyond the ancient eastern mole shows no low energy harbour facies. The harbour basin was therefore not more extensive in this direction. Eighteenth to nineteenth century gravures clearly show this ancient breakwater and city wall transformed into living quarters (Fig. 18). Our findings corroborate drawings made by Poulain de Bossay [51,52] and Renan [58], who were the first to recognise the silting-up of the northern harbour since antiquity (Figs. 19 and 20).

6. Conclusion

The palaeogeography of Tyre's northern harbour has been fashioned since antiquity by overriding geomorphological and mareographic forcing factors. During the Bronze Age, Tyre was characterised by a semi-open marine cove used as a proto-harbour by early settlers and mariners. After the 1st millennium BC, rising sea levels and expanding international trade forced the Phoenicians to build early artificial harbour infrastructure, before the later apogees of the Roman and Byzantine periods. Problems of rapid silting were

Fig. 20. Renan's proposed northern harbour extension in antiquity, marked in grey (From Renan, p. 569). Dotted lines mark the present coastline.

overcome during the latter periods by repeated phases of dredging, with deliberate overdeepening and removal of earlier harbour sediment strata to maintain a navigable harbour depth. The economic demise of Tyre after the Byzantine period is represented by sediment infilling and coastal progradation.

The nature of Tyre's landscape evolution offers a unique opportunity for maritime archaeology. Given the outstanding preservation properties of the fine-grained sedimentary context, coupled with the presence of the water table, scope for future archaeological work in this Levantine harbour is exceptional. Fine-grained sediment means the heart of the Bronze Age, Phoenician, Greek, Roman and Byzantine ports could be excavated on land, in much the same way as a classic terrestrial dig. We suggest a program of management be developed for this important cultural site, with clearly defined scientific, protection, public awareness and education objectives.

Acknowledgements

The authors wish to thank the AIST (M. Chalabi) for generously funding the radiocarbon dates. The team would also like to thank the DGA. This research was undertaken within the framework of the programs CEDRE F60/L58 and UNESCO CPM 700.893.1. N. Marriner has benefited from an Entente Cordiale scholarship (2004 5052) and Leverhulme Study Abroad Studentship (SAS/2005/4/0032).

References

[1] I. Abd-el-Al, Le Litani, étude hydrologique, Service Hydraulique de le République Libanaise, Beirut, 1948.

[2] H.A. Amery, The Litani River of Lebanon, The Geographical Review 83 (3) (1993) 229–237.

[3] A. Barash, Z. Danin, Fauna Palaestina, mollusca I. Annotated list of Mediterranean molluscs of Israel and Sinai, The Israel Academy of Sciences and Humanities, Jerusalem, 1992.

[4] E. Bard, B. Hamelin, M. Arnold, L. Montaggioni, G. Cabioch, G. Faure, F. Rougerie, Deglacial sea-level record from Tahiti corals and the timing of global meltwater discharge, Nature 382 (1996) 241–244.

[5] D. Bellan-Santini, J.C. Lacaze, C. Poizat, Les biocénoses marines et littorales de Méditerranée, Coll. Patrimoines Naturels (19), Muséum National d'Histoire Naturelle, 1994.

[6] Z.R. Beydoun, Observations on geomorphology, transportation and distribution of sediments in western Lebanon and its continental shelf and slope regions, Marine Geology 21 (1976) 311–324.

[7] P. Bikai, The Pottery of Tyre (ancient Near East), Aris & Phillips, Oxford, 1979.

[8] P. Bikai, P. Bikai, Tyre at the End of the Twentieth Century, Berytus 35 (1987) 67–96.

[9] G. Bitar, S. Kouli-Bitar, Inventaire des mollusques marines benthiques du Liban et remarques biogéographiques sur quelques espèces nouvellement signalés, Mesogée 56 (1998) 37–44.

[10] S. Bottema, Evaluation of Climate Proxy Data in Relation to the European Holocene, in: B. Frenzel, A. Pons, B. Gläser (Eds.), Gustav Fischer, Stuttgart, 1991.

[11] L. Brochier, Etude de la sedimentation anthropique, La stratégie des ethnofacies sédimentaires en milieu de constructions en terre, BCH 118 (1994) 619–645.

[12] R.W.H. Butler, S. Spencer, H.M. Griffiths, in: R.E. Holdsworth, R.A. Strachan, J.F. Dewey (Eds.), Continental Transpressional and Transtensional Tectonics, Geological Society Special Publications 135, London, 1998.

[13] Z. Carmel, D.L. Inman, A. Golik, Characteristics of storm waves off the Mediterranean coast of Israel, Coastal Engineering 9 (1985) 1–19.

[14] Z. Carmel, D.L. Inman, A. Golik, Directional wave measurement at Haifa, Israel, and sediment transport along the Nile littoral cell, Coastal Engineering 9 (1985) 21–36.

[15] M. Chehab, Fouilles de Tyr, Bulletin du Musée de Beyrouth 33–36 (1983–1986).

[16] F. Cimerman, M.R. Langer, Mediterranean foraminifera, Slovenska akademija znanosti in umetnosti, Ljubljana (1991).

[17] L. Dubertret, Carte géologique du Liban au 50.000°, Feuille de Tyr-Nabatiyé et Naqoura-Bennt Jbail, Institut Géographique National, Beirut, 1961.

[18] M. El Amouri, M. El Helou, M. Marquet, I. Nourredine, M. Seco Alvarez, Mission d'expertise archéologique du port sud de Tyr, sud Liban: résultats préliminaires, Bulletin d'Archéologie et d'Architecture Libanaises (in press).

[19] R.G. Fairbanks, A 17,000-year glacio-eustatic sea-level record: influence of global melting rates on the Younger Dryas event and deep-ocean circulation, Nature 342 (1989) 637–642.

[20] K. Fleming, P. Johnston, D. Zwartz, Y. Yokoyama, K. Lambeck, J. Chappell, Refining the eustatic sea-level curve since the Last Glacial Maximum using far- and intermediate-field sites, Earth and Planetary Science Letters 163 (1998) 327–342.

[21] R.L. Folk, A review of grain-size parameters, Sedimentology 6 (1966) 73–93.

[22] H. Frost, in: V. Karageorghis, D. Michaelides (Eds.), Proceedings of the International Symposium 'Cyprus and the Sea', University of Cyprus, Nicosia, 1995.

[23] H. Frost, Recent observations on the submerged harbour-works at Tyre, Bulletin du Musée de Beyrouth XXIV (1971) 103–111.

[24] H. Frost, Archaeology, history and the history of archaeology connected with Tyre's harbour, Bulletin d'Archéologie et d'Architecture Libanaises (in press).

[25] J.-P. Goiran, C. Morhange, Géoarchéologie des ports antiques de méditerranée, Topoi 11 (2003) 645–667.

[26] J.-P. Goiran, C. Morhange, M. Bourcier, P. Carbonel, C. Morigi, Evolution des rivages d'Alexandrie à l'Holocène récent, marge occidentale du delta du Nil, Egypte, Méditerranée 94 (2000) 83–90.

[27] V. Goldsmith, S. Sofer, Wave climatology of the southeastern Mediterranean, Israel Journal of Earth Science 32 (1983) 1–51.

[28] P. Hallock, in: B.K. Sen Gupta (Ed.), Modern Foraminifera, Kluwer Academic Publishers, Dordrecht, 1999.

[29] L. Hottinger, E. Halicz, Z. Reiss, Recent Foraminiferida From the Gulf of Aqaba, Red Sea, Slovenska akademija znanosti in umetnosti, Ljubljana (1993).

[30] H.J. Katzenstein, The History of Tyre, Goldberg Press, Jerusalem, 1997.

[31] H.J. Katzenstein, Tyre in the early Persian period (539–486 B.C.E.), Biblical Archaeologist 42 (1979) 23–34.

[32] B. Kjerfve, in: D.A. Wolfe (Ed.), Estuarine variability, Academic Press, Orlando, 1986.

[33] J.C. Kraft, G.R. Rapp, I. Kayan, J.V. Luce, Harbor areas at ancient Troy: Sedimentology and geomorphology complement Homer's Iliad, Geology 31 (2003) 163–166.
[34] J. Laborel, F. Laborel-Deguen, Biological indicators of relative sea-level variations and co-seismic displacements in the Mediterranean region, Journal of Coastal Research 10 (1994) 395–415.
[35] E. Marcus, in: E.C.M. van der Brink, T.F. Levy (Eds.), Egypt and the Levant, Interrelations from the 4th Through the Early 3rd Millennium BCE, Continuum International Publishing Group, London, 2002.
[36] E. Marcus, personal communication.
[37] N. Marriner, C. Morhange, I. Rycx, M. Boudagher-Fadel, M. Bourcier, P. Carbonel, J.-P. Goiran, G. Noujaim-Clark, Holocene coastal dynamics along the Tyrian peninsula, south Lebanon; The palaeo-geographical evolution of the northern harbour, Bulletin d'Archéologie et d'Architecture Libanaises (in press).
[38] I. Mazzini, P. Anadon, M. Barbieri, F. Castorina, L. Ferreli, E. Gliozzi, M. Mola, E. Vittori, Late quaternary sea-level changes along the Tyrrhenian coast near Orbetello (Tuscany, central Italy): palaeoenvironmental reconstruction using ostracods, Marine Micropaleontology 37 (1999) 345–364.
[39] C. Morhange, Mobilité littorale de quelques sites portuaires antiques de Méditerranée, Marseille, Pouzzoles, Cumes, Kition et Sidon, Habilitation à Diriger des Recherches, Université de Provence, CEREGE, Aix-Marseille, 2001.
[40] C. Morhange, F. Blanc, M. Bourcier, P. Carbonel, A. Prone, S. Schmitt-Mercury, D. Vivent, A. Hesnard, Bio-sedimentology of the late Holocene deposits of the ancient harbor of Marseilles (Southern France, Mediterranean sea), The Holocene 13 (2003) 593–604.
[41] C. Morhange, K. Espic, C. Doumet-Serhal, M. Bourcier, P. Carbonel, The ancient harbours of Sidon, attempt at a synthesis (1998–2002), Archaeology and History in Lebanon 18 (2003) 71–81.
[42] C. Morhange, P.A. Pirazzoli, D. Chardon, N. Marriner, L.F. Montaggioni, T. Nammour, Late Holocene relative sea-level changes and coastal tectonics in Lebanon, Eastern Mediterranean, Quaternary Science Reviews (in press).
[43] J.W. Murray, Distribution and Ecology of Living Benthic Foraminiferids, Heinemann Educational Books Limited, London, 1973.
[44] Y. Nir, The city of Tyre, Lebanon and its semi-artificial tombolo, Geoarchaeology 11 (1996) 235–250.
[45] I. Noureddine, M. Helou, Underwater archaeological survey in the northern harbour at Tyre, Bulletin d'Archéologie et d'Architecture Libanaises (in press).
[46] J.-M. Péres, J. Picard, Nouveau manuel de bionomie benthique de la mer Méditerranée, Recueil des Travaux de la Station Marine d'Endoume 31 (1964) 1–137.
[47] A. Poidebard, Un grand port disparu, Tyr. Recherches aériennes et sous-marines, 1934–1936, Librairie Orientaliste Paul Geuthner, Paris, 1939.
[48] P. Pomey, Les épaves grecques et romaines de la place Jules Verne à Marseille, Comptes-Rendu de l'Académie des Inscriptions et Belles Lettres 2 (1995) 459–482.
[49] G.T. Poppe, Y. Goto, European seashells, vol. I, Verlag Christa Hemmen, Wiesbaden, 1991.
[50] G.T. Poppe, Y. Goto, European seashells, vol. I, Verlag Christa Hemmen, Wiesbaden, 1993.
[51] P.A. Poulain de Bossay, Recherches sur la topographie de Tyr, Madame Maire-Nyon, Paris, 1861.
[52] P.A. Poulain de Bossay, Recherches sur Tyr et Palaetyr, Extrait du recueil de géographie, Paris, 1863.
[53] A. Raban, in: V. Karageorghis, D. Michaelides (Eds.), Proceedings of the International Symposium 'Cyprus and the Sea', University of Cyprus, Nicosia, 1995.
[54] A. Raban, Conceptual Technology of Phoenician Harbours in the Levant, Actas del Congreso Internacional de Estudios Fenicios y Púnicos, Universidad de Cádiz, Cádiz, 1995.
[55] P.J. Reimer, F.G. McCormac, Marine radiocarbon reservoir corrections for the Mediterranean and Aegean seas, Radiocarbon 44 (2002) 159–166.
[56] E.G. Reinhardt, R.T. Patterson, C.J. Schröder-Adams, Geoarchaeology of the ancient harbor site of Caesarea Maritima Israel: evidence from sedimentology and paleoecology of benthic foraminifera, Journal of Foraminiferal Research 24 (1994) 37–48.
[57] E.G. Reinhardt, A. Raban, Destruction of Herod the Great's harbor Caesarea Maritima, Israel, geoarchaeological evidence, Geology 27 (1999) 811–814.
[58] E. Renan, La Mission de Phénicie, Imprimerie Nationale, Paris, 1864.
[59] E. Ribes, D. Borschneck, C. Morhange, A. Sandler, Recherche de l'origine des argiles du bassin portuaire antique de Sidon, Archaeology and History in Lebanon 18 (2003) 82–94.
[60] H. Ron, Deformation along the Yammuneh, the restraining bend of the Dead Sea transform: paleomagnetic data and kinematic implications, Tectonics 6 (1987) 653–666.
[61] D.S. Rosen, Assessment of marine environmental impacts due to construction of artificial islands on the coast of Israel; Characterisation of mete-oceanographic climate in the study sector, National Institute of Oceanography, Haifa, 1998.
[62] A.M. Samir, H.F. Abdou, S.M. Zazou, W.H. El-Menhaway, Cluster analysis of recent benthic foraminifera from the northwestern Mediterranean coast of Egypt, Revue de Micropaléontologie 46 (2003) 111–130.
[63] A. Sandler, B. Herut, Composition of clays along the continental shelf of Israel: contribution to the Nile versus local sources, Marine Geology 167 (2000) 339–354.
[64] P. Sanlaville, Etude géomorphologique de la région littorale du Liban, Publications de l'Université Libanaise, section des études géographiques, Beirut, 1977.
[65] H. Sayegh, J. Elayi, Rapport préliminaire sur le port de Beyrouth au Fer III/Perse (Bey 039), Transeuphratène 19 (2000) 65–73.
[66] G. Siani, M. Paterne, E. Michel, R. Sulpizio, A. Sbrana, M. Arnold, G. Haddad, Mediterranean sea surface radiocarbon reservoir age changes since the last glacial maximum, Science 294 (2001) 1917–1920.
[67] D.J. Stanley, Y. Mart, Y. Nir, Clay mineral distributions to interpret Nile Cell provenance and dispersal: II. Coastal plain from Nile delta to Northern Israel, Journal of Coastal Research 13 (1997) 506–533.
[68] M. Stuiver, T.F. Braziunas, Modelling atmospheric ^{14}C influences and ^{14}C ages of marine samples to 10,000 BC, Radiocarbon 35 (1993) 137–189.
[69] M. Stuiver, P.J. Reimer, T.F. Braziunas, High-precision radiocarbon age calibration for terrestrial and marine samples, Radiocarbon 40 (1998) 1127–1151.
[70] C.D. Walley, Some outstanding issues in the geology of Lebanon and their importance in the tectonic evolution of the Levantine region, Tectonophysics 298 (1998) 37–62.
[71] Y. Yasuda, H. Kitagawa, T. Nakagawa, The earliest record of major anthropogenic deforestation in the Ghab Valley, northwest Syria: a palynological study, Quaternary International 73/74 (2000) 127–136.